siam

16th Annual Meeting of the Bulgarian Section of SIAM
December 21 – 23, 2021
Sofia

BGSIAM'21

EXTENDED ABSTRACTS

16th Annual Meeting of the Bulgarian Section of SIAM
December 21 – 23, 2021, Sofia

BGSIAM'21 Extended abstracts

ISSN: 1313-3357 (print)
ISSN: 1314-7145 (electronic)

Printed in Sofia, Bulgaria

PREFACE

The Bulgarian Section of SIAM (BGSIAM) was formed in 2007 with the purpose to promote and support the application of mathematics to science, engineering and technology in Republic of Bulgaria. The goals of BGSIAM follow the general goals of SIAM:

- To advance the application of mathematics and computational science to engineering, industry, science, and society;
- To promote research that will lead to effective new mathematical and computational methods and techniques for science, engineering, industry, and society;
- To provide media for the exchange of information and ideas among mathematicians, engineers, and scientists.

During BGSIAM'21 conference a wide range of problems concerning recent achievements in the field of industrial and applied mathematics will be presented and discussed. The meeting provides a forum for exchange of ideas between scientists, who develop and study mathematical methods and algorithms, and researchers, who apply them for solving real life problems.

The strongest research groups in Bulgaria in the field of industrial and applied mathematics, advanced computing, mathematical modelling and applications will be presented at the meeting according to the accepted extended abstracts. Many of the participants are young scientists and PhD students.

LIST OF INVITED SPEAKERS:

- Clemens Hofreither (Johann Radon Institute for Computational and Applied Mathematics, Linz, Austria)
  "Recent advances in rational approximation methods for fractional diffusion"
- Julius Kaplunov (Keele University,UK)
  "An asymptotic theory for a functionally graded plate"
- Svetozar Margenov (Bulgarian Academy of Sciences)
  "Achievements and challenges in numerical methods for multidimensional spectral fractional diffusion problems"

The present volume contains extended abstracts of the presentations (Part A) and list of participants (Part B).

Ivan Georgiev
Chair of BGSIAM Section

Hristo Kostadinov
Vice-Chair of BGSIAM Section

Elena Lilkova
Secretary of BGSIAM Section

Sofia, December 2021

Table of Contents

Part A

Extended abstracts[1]

[1] Arranged alphabetically according to the family name of the first author.

Watermarking Audio Content: Data embedding based on Fast Fourier Transform

T. Alexandrova, H. Kostadinov, N. Manev

The possibility of embedding watermarks robust against compression in musical audio files is investigated in this paper. The compression itself can be considered as a communication channel whose statistical characteristics are sensitive to the compressed musical genre. We study the compression format Advance Audio Coding (AAC) and collect statistical data for different musical genres. AAC is designed to be the successor of the MP3 format and it generally achieves better sound quality than MP3 format at the same bit rate. AAC is the default audio format for the most modern devices and platforms that dominates in recent years.

The process of embedding and retrieving a watermark can be regarded as a binary communication channel. In our previous work we investigated an embedding method based on wavelet transformation of the target audio file. In this work we replace the wavelet transformation with Fast Fourier Transform preserving other stages of investigation unaffected.

We are going to make a comprehensive investigation of an embedding technique applied to musical files which will be subject of subsequent AAC compression. We aim to propose a method of choosing embedding parameters so that to achieve acceptable probability of errors without perceptible loss of quality of the audio file.

References

[1] B. Chen and G.W. Wornell, Quantization index modulation: A class of provably good methods for digital watermarking and information embedding, IEEE Trans. on Information Theory, vol. 47 no.4, pp. 1423–1443, 2001.

[2] R. Martinez-Noriega, M. Nakano, B. Kurkoski, and K. Yamaguchi, High Payload Audio Watermarking: toward Channel Characterization of MP3 Compression, Journal of Information Hiding and Multimedia Signal Processing, vol. 2, no. 2, 91-107, (2011).

Residual Bounds of a Class of Nonlinear Matrix Equations

V. Angelova

We consider the nonlinear complex matrix equation

$$X^p = A + M(B + X^{-1})^{-1}M^*, \quad p \geq 1, \tag{1}$$

where X, A, B and M are complex $n \times n$ matrices. X is the Hermitian positive definite solution; the data matrices A and B are Hermitian positive semi-definite, and M is an arbitrary matrix. The exponent $p \geq 1$ is a positive integer number. M^* denotes the complex conjugate transpose of the matrix M. For this equation, necessary condition for the existence of its Hermitian positive definite solution and an elegant estimate of the solution, as well as one fixed-point iteration method and one inversion-free variant iteration method for obtaining the positive definite solution are derived by Meng and Kim in [J. Meng and H-M. Kim. The positive definite solution of the nonlinear matrix equation $X^p = A+M(B+X^{-1})^{-1}M^*$. *Compt Appl Math*, 322:139–147, 2017]. Local and nonlocal perturbation bounds for the computed solution X to equation (1) are proposed in [V.A. Angelova. Sensitivity of the nonlinear matrix equation $X^p = A + M(B + X^{-1})^{-1}M^*$. In *Proc. of extended abstracts 15th Annual Meeting of the Bulgarian Section of SIAM*, page 3, Sofia, Bulgaria, December 15-17, 2020].

The matrix equation (1) is a generalized version of the discrete-time algebraic Riccati equation $X = MX(I+BX)^{-1}M^*+A$, which has wide application in control and systems theory, dynamic programming, stochastic filtering, ladder network. In addition, setting $p = 1$ and replacing $B = 0$ and $M = M^*$, equation (1) is simplified to the well known from signal processing, systems and control theory, discrete-time algebraic Lyapunov equation /or Hermitian Stein equation/ $X = M^*XM + A$. Generalizations of equation (1) are the nonlinear complex matrix equations $X^s \pm A^*X^tA = Q$, $A_0 + \sum_{i=1}^{k} \sigma_i A_i^* X^{p_i} A_i = 0$, $\sigma_i = \pm 1$ and $C + \sum_{i=1}^{r} A_i X B_i - D X^s E = 0$.

In this paper, we extend the knowledge on the sensitivity of equation (1) deriving residual bounds for its approximate solution, computed by a numerically stable iterative algorithm. The residual bound is a useful criteria for judging whether the approximation of the computed solution is acceptable for terminating the iterative algorithm. The bounds proposed in the paper are limited to terms of second order and are obtained, applying the techniques of the Fréchet derivatives, the method of Lyapunov majorants and the Schauder fixed point principle. A numerical example shows the efficiency of the bounds proposed in a wide range of values for the exponent p. Useful facts on the affine approximation of the matrix rational power function $A \to A^p$ are proved as well.

Acknowledgments This work is accomplished with the partial support by the Grant BG PLANTNET "Establishment of national information network genbank – Plant genetic resources".

Parameter Identification Analysis of Food and Population Dynamics in Honey Bee Colonies

A. Z. Atanasov, S. G. Georgiev, L. G. Vulkov

Honeybees play indispensable and important roles in human life, economy, and agriculture. For example, honeybees not only produce valuable products, such as honey, royal jelly, bee wax and propolis for the market, but also are responsible for pollinating crops such as blueberries, cherries and almonds, that is worth $ 215 billion annually worldwide. Unfortunately, honeybee population has been decreasing globally. In the United States, the total number of honey bee colonies has been reduced approximately 40 percent to 50 percent, while in the rest of the world the total number of colonies is reduced by 5 percent to 10 percent.

The important and critical causes for honeybee colony mortalities include disease, land-use change, pesticides, pathogens, parasites, and poor beekeeping management. One of the most used in practice and the theory mathematical model of honey bee population is proposed in Khoury et al. It only includes the adult bees, which are divided into two classes: hive bees and foragers. It is assumed that the rate that adults emerged from pupation is a function of hive size only and that food is not a limiting factor in the hive population dynamics. It is also assumed that the hive had sufficient available food so that food scarcity did not affect the population dynamics. In the next papers of Khoury et al, [1, 2], they extended this model to include both **food** and brood explicitly. Let B be the number of uncapped brood in the hive, H be the number of hive bees and F the number of foragers. Let f be a measure of the amount of food that is stored in the hive and available for the colony to use. We assume that the survival of uncapped brood (eggs and larvae) is dependent on the number of hive bees available to tend and feed brood, on food availability and on the laying rate L of the queen. Adult bees emerge 12 days after pupation and it is assumed that the mortality of capped brood is negligible. Foragers are recruited from the hive bee class and die at a rate m. Let t be the time in days. Then the whole process is described as a system of four differential equations:

$$\frac{\mathrm{d}B}{\mathrm{d}t} = L.S(f,H) - \phi B \equiv g_1(B,f,H), \tag{1}$$

$$\frac{\mathrm{d}f}{\mathrm{d}t} = cF - \gamma_B B - \gamma_H H - \gamma_F F \equiv g_2(B,H,F), \tag{2}$$

$$\frac{\mathrm{d}H}{\mathrm{d}t} = \phi B(t-\tau) - H.R(f,H,F) \equiv g_3(B,f,H,F), \tag{3}$$

$$\frac{\mathrm{d}F}{\mathrm{d}t} = H.R(f,H,F) - mF \equiv g_4(f,H,F). \tag{4}$$

The survival brood function $S(f,H)$ at the assumption that it becomes constant as f and H become large, is taken as follows

$$S(H,f)=\frac{f^2}{f^2+b^2}\cdot\frac{H}{H+v}, \tag{5}$$

where b and v are constant parameters that determine how rapidly $S(f,H)$ tends to one as f and H increase, respectively. The first multiplier in (5) models the way that the brood survival declines when food stores are low. This decline in brood survival has two causes: brood dies because there is not enough food to feed them as they develop, and because workers cannibalize the eggs and young larvae when food is scarce to recycle protein in the colony and so increase the likelihood of older larvae surviving to pupation.

In the equation (3), the term $\phi B(t-\tau)$ is the rate that adult bees emerge from pupation. The bees that are emerging at time t are the same bees that entered pupation at $t-\tau$. The function $R(f,H,F)$ gives the proportional rate that hive bees make the transmission into foragers.

The recruitment function is suggested as follows

$$R(f,H,F)=\alpha_{\min}+\alpha_{\max}\left(\frac{b^2}{b^2+f^2}\right)-\sigma\left(\frac{F}{F+H}\right), \tag{6}$$

where $\alpha_{\min}$ is the rate that hive bees become foragers when there is a plenty of stored food but no foragers in the hive, $\alpha_{\max}$ governs the strength of the effect that low food stores have on the transition to foragers and b controls the rate that the food-dependent terms decrease as food stores increase. Social inhibition depends on the proportion of the foragers in the adult population and the strength of this inhibition is governed by σ.

In the equation (2) c is the average amount of food collected per forager per day and is assumed that it is constant. The consumption of stored food by brood, hive bees and foragers is given by γ_B, γ_H and γ_F, respectively.

Let all solutions $\{B(t;\mathbf{p}),f(t,\mathbf{p}),H(t;\mathbf{p}),F(t;\mathbf{p})\}$, $\mathbf{p}\equiv(p^1=\gamma_B,p^2=\gamma_H,p^3=\gamma_F)$ be defined on the interval $t_0\le t\le t_{\rm f}$ given the initial conditions

$$B(t_0)=B^0,\quad f(t_0)=f^0,\quad H(t_0)=H^0,\quad F(t_0)=F^0. \tag{7}$$

To find the unknown parameters $\mathbf{p}$, we minimize the following cost functional:

$$J(\mathbf{p})=\sum_{k=0}^{K_B}(B(t_k)-U_k)^2+\sum_{k=0}^{K_f}(f(t_k)-X_k)^2+\sum_{k=0}^{K_H}(H(t_k)-Y_k)^2+\sum_{k=0}^{K_F}(F(t_k)-Z_k)^2, \tag{8}$$

where the known functions $U(t_k),X(t_k),Y(t_k),Z(t_k)$ are the observed quantities in practise.

We minimize the error functional (8) via the adjoint equation optimization approach.

References

[1] D.S. Khoury, A.B. Barron, M.R. Myerscough, Modelling food and population dynamics in honey bee colonies, PLoS ONE 8: e59084, (2013).

[2] M.R. Myerscough, D.S. Khoury, S. Ronzani, A.B. Barron, Why do hives die? Using mathematics to solve the problem of honey bee colony collapse, In: B. Andersen et al, The Role and Importance of Mathematics in Innovation, Mathematics for Industry, 25, (2017).

The Randomness in Shared Web Hostings

I. Blagoev, T. Balabanov, I. Iliev

Introduction The World Wide Web has been the most used Internet service for the past three decades. In its base are group of protocols - TCP/IP and HTTP. When used in their basic form, they do not provide any security for encryption. If the data needs to be transferred securely, the TLS tunnel protocol takes action. TLS at the packet level envelops the data transmitted in pure form. The level of security is determined by a set of cryptographic algorithms. Asymmetric cryptography is used and the quality of the random numbers is the basis of the security.

Secure Communication As a base of secure communication, TLS runs in two phases - hand- shake and channel establishment via session key. Random numbers exchange take place between the server and the client during the handshake phase. The randomness of these numbers is extremely important for the asymmetric encryption of information. The efficiency of the random numbers is measured by the degree of entropy [1]. The quality of the random numbers depends on the shared web hosting organization. Platforms of this type share the entire hardware resource between many users and their web service applications [2].

Public Hosting Service Survey The survey was done on the following services - IP address; TCP ports; Web service; cPanel service; DNS administration panel; Mail service. A special Python script has been written to establish a TLS connection as a client. During the TLS handshake phases, the data from the remote random number generator has been extracted. The open-source software Dieharder has been used for quality estimation of the collected random numbers. From a total of 114 tests, only 25 had good level of randomness, 76 had compromised or predictable value and 13 were vulnerable.

Conclusions As a result of the investigation, from a set of public web services, it can be con- cluded that the level of cybersecurity is not desirable when there are systems with critical functionality and/or systems for processing personal data. In real-life practice, it is better to provide hosting on our own server or a leased VPS, where the number of concurrent systems will not exceed the capabilities of the shared system resources used to secure the cryptography.

Acknowledgments This research is partially supported by the Bulgarian Ministry of Education and Science (contract D01–205/23.11.2018) under the National Scientific Program "Information and Communication Technologies for a Single Digital Market in Science, Edu- cation and Security (ICTinSES)", approved by DCM # 577/17.08.2018.

References

[1] Blagoev I.: Method for Evaluating the Vulnerability of Random Number Generators for Cryptographic Protection in Information Systems. Proceedings of Advanced in High Per- formance Computing (HPC'19). Studies in Computational Intelligence, vol. 902. Springer, Cham. https://doi.org/10.1007/978-3-030-55347-0 33 (2021)

[2] Blagoev I.: Neglected Cybersecurity Risks in the Public Internet Hosting Service Providers. Information & Security Journal, vol. 47, no. 1, 62-76. https://doi.org/10.11610/isij.4704 (2020)

Forecasting Models for the House Price Index in Bulgaria

V. Boutchaktchiev

The House Price Index (HPI) is produced by the National Statistical Institute (NSI) since 2005, first on an national levels and later, since 2015, on a regional level. In this study we use the national data, as well, as the data for the metropolitan areas of the six largest cities in the country: Sofia, Plovdiv, Varna, Rousse, Bourgass and Stara-Zagora. It is a tool which is designed to measure the expenditure of the population for residential real estate.
The task of forecasting future levels of the HPI arises with the introduction of a new accounting standard, IFRS9, to the Bulgarian banks. Since 2018, the banks are required to statistically estimate the future value of houses used as collateral for loans. The nature of estimation of Expected Credit Loss requires the evaluation of the HPI one and more years ahead based on currently available economic indicators. (Cf., e.g., [1].)
We study several specifications of forecasting models, to verify the corelation of HPI with other financial and economic indicators, as previosly documented by the literature in the field. (Cf., e.g., [2].)
We find the following conclusions:

1. We develop an original instrumental-variable model forecasting the house price index (HPI), confirming its correlation with various indicators, including real-estate market demand, construction industry business cycle and general macroeconomic environment.

2. The general conclusion was, however, that the two most prominent drivers of HPI remain the interest rates and the internal inertia of the RE market. The best-fitting specification requires the estimation a hybrid autoregressive model.

Acknowledgment This work has been supported in part by UNWE Research Program (Research Grant No. 17/2021.)

References

[1] Gaffney, E., R. Kelly, and F. McCann, (2014), *A transitions-based framework for estimating expected credit losses*, Research Technical Papers 16/RT/14, Central Bank of Ireland.
[2] Nagaraja, C. H., Brown, L. D., and Wachter, S. M. (2010). House Price Index Methodology. *UPenn Wharton School Statistics Papers* `https://repository.upenn.edu/statistics_papers/145`

Knowledge – Material Science in Medicine

S. Bushev

HUMAN BODY – SYSTEMS [1]: ***Skeletal*** anatomy (Anterior and Posterior view); ***myology*** – muscles (Terrisodres); ***circulation lymphatique; Internal Human Organs***: brain, eyes, ears, heart, lungs, esophagus, stomach, kidneys, bladder, urethra, male, female, small and large intestines, pancreas, liver; ***Circulatory system (angiology*** – venous and arterial blood); ***Nervous*** system.

Methodology [2, 3, 4, 5, 6 and 7] : I. From [2] Heuristic approaches to solving scientific problems; Submicroparticles and mega world [2]; a new possibility for relationships between them [2] i.e. we use a ***multi-scale approach***; and the end the logical formulation of physical laws is of the type $\Pi_{(x)}\left[W\left(x\right)\rightarrow Z\left(x\right)\right]$, where $W\left(x\right)$ is a description of conditions; $Z\left(x\right)$ is the physical relationship between several parameters [2]; if Z changes it is a new law; if W changes, it is a new wording of the same law; **II**. Thermodynamics system [3]: second law: Kelvin: an impossible process with the end result in the conversion of heat taken from a source with the same temperature, i.e. there is no change in the system; Clausius: not a possible process, heat transfer from a colder body to a warmer body; system [3]: entropy or an infinitesimal process is $dS=dQ/T$ and $S\left(A\right)=\int_{0}^{A}dQ/T$, and the Boltzmann ratio is $\mathbf{S}=\mathbf{kln}\boldsymbol{\pi}$, where $\boldsymbol{\pi}$ is probabilities [3]; Phase space of the system is the set $\left(-\infty^{2f}\right)$, where f is the number of degrees of freedom; Nernst's theorem [3]: *At absolute zero, the dynamic state of the system corresponds to only one state: the lowest energy compatible with a given crystal structure or a given state of matter [3]. Arbitrariness in the relationship between* $\boldsymbol{\pi}$ *and* $\boldsymbol{S}$ *in a classical interpretation, is removed using the principles of quantum mechanics by discretizing the phase space of cells with volume* $\hbar^{f}$*, where* $\hbar$ *is Plank's const (*$\hbar$*=1.054571817...*$\times10^{\breve{}34}$ *Js) [3]; f number of degrees of freedom.* **III**. Open thermodynamics system (OTS) [4]: extend form secon law of **I. Prigogine of OTS** is the sum $\mathbf{dS/dt}=\mathbf{dS_{E}/dt}+\mathbf{dS_{I}/dt}$, where dS_{E}/dt entropy flow from the system/environment interaction, and dS_{I}/dt is entropy obtained in the system from *irreversible processes* [4]. Consequences [4]: $dS_{I}/dt\geq0$, if $dS_{I}/dt=0\Rightarrow$ equilibrium; at $dS_{E}/dt=0\Rightarrow$ isolated system $dS/dt=dS_{I}/dt\geq0$. The entropy term dS_{E}/dt is the difference between ***an open*** and a ***closed*** system. Always $dS_{I}/dt\neq0$; and dS_{E}/dt there is no definite sign. This allows us *to present evolution as a process in which the system reaches a lower entropy than the beginning [4]:* $\Delta S=\int\limits_{on\,way}dS<0$; this condition is unlikely, but can take place indefinitely provided the system reaches a steady state in which $dS/dt=0$ or $dS_{E}/dt=\breve{}dS_{I}/dt<0$ which is possible with a large negative entropy flow and it is possible to maintain some orderly configuration i.e. we have the principle: imbalance can be a source of order; **IV.** Sustainability of (OTS) [6] i.e. physical system is not destroyed; **V.** Controlability [6 and 7]: in order to be resistant to destroying an engineering system it is necessary to have the property of controlability, i.e. OTC parameters to be changed for control. Multi–scale mathematical and mathematical physics description of **human body** is:

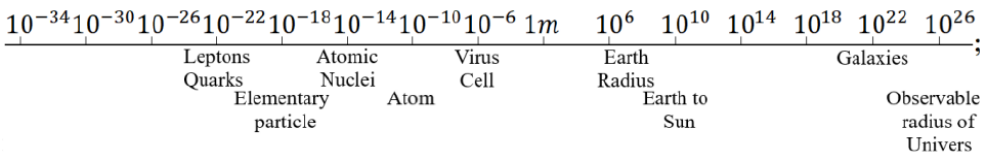

and next tasks

SCHRÖDINGER EQUATIONS [5]

$$-\frac{\hbar^2}{2m}\Delta\Psi\left(x,y,z,t\right)+U\left(x,y,z,t\right)\Psi\left(x,y,z,t\right)=i\hbar\frac{\partial\Psi\left(x,y,z,t\right)}{\partial t},\ (non-stationary)$$

$$\Delta\Psi\left(x,y,z\right)+\frac{2m}{\hbar^2}\left[E-U\left(x,y,z\right)\right]=0,\quad (stationary)$$

STEFAN's TASK [6,7]

$$c_i\rho_i\frac{\partial T_i}{\partial x}=\lambda_i\frac{\partial^2 T_i}{\partial x^2},\ i=S;L \tag{1}$$

$$\lambda_S G_S-\lambda_L G_L=\rho_S Q_m R, \tag{2}$$

$$T_L\left(x,t=0\right)=const,\ for x\in\left(0\div\infty\right) \tag{3}$$

$$T_0=T_L\left(x=0,t=0\right),\ and$$

$$T_0=T_S\left(x=0,t\right) \tag{4}$$

And the end general principle of OTS control [6]: Control on account of information about the external effect on technological object feedback main processes (from indirect information carrier).

We present everything presented to us to use the well-known concept of **synergetics**, which according to H. Haken is: *unification of sciences*. Between 32,000 and 35,000 chemical reactions take place in the human body in a very short time $\mathbf{\Delta t}$ *accepted as a basic scale unit*! When using full knowledge, times $\mathbf{t}\ll\mathbf{\Delta t}$ can be used for example $\mathbf{t}<10^{-45}$ sec and less. This goes to the description of objects much smaller than the cell.

We understand materials science in medicine: prostheses, for example, nitrogen steel has been created at the institute and its prostheses have a very good tissue susceptibility to the human body; 3D printer for obtaining soft tissues in the human body.

References

[1] H. Brundle, Human body infografics, BookLife Publishing Ltd. Norfolk. ISBN: 978-1-83927-324-7; H. Baum, The amazing human body.

[2] A. Polikarov, Methodology of scienific knowledge, Science and Art, Sofia, 1972.

[3] E. Fermi, Thermodynamics, second stereotypical edition, Kharkov University Press, 1973. (In Russian).
[4] G. Nikolis, I. Prigogine, Knowledge of the complex, Mir, Moscow, 1990. (In Russian).
[5] Ch. Wert, R. Thomson, Physics of Solids, Peace, Moscow (1969). (In Russian).
[6] S. M. Bushev, PhD dissertation:Controlability Problemof Crystallization Process in Casting, Sofia, TU – Sofia, 1993.
[7] S. Bushev, V. Georgiev, Developing the Solution of Stefans's Problem, Comptes rendus de l'Academié bulgare des Sciences, Tome 47, No 3, p.9-12,1994.

Local Geometry of Different Grafting Schemes of the CP4-Derived Linear Peptide onto Knotted Scaffolding

Y. Cheng, X. Peng, P. Petkov, N. Ilieva

Cyclotides are special knotted peptides stabilized by three pairs of disulfide bonds. With such a molecule as the scaffold, small peptides can be grafted onto it, thus engineering some specific conformations and functions. It has been shown that MCoCP4, formed by the peptide CP4 (CLATWAVG) grafted on loop 6 of the cyclotide MCoTI-I, can reduce the cytotoxicity of α-synuclein and, hence, has potential to inhibit the Parkinson Disease. In this study, we analyze the dynamical and geometrical properties of this specific grafted molecule based on molecular dynamics (MD) simulations. By visualizing the local geometry in a discrete Frenet frame (DFF) along the trajectory, we locate several stable segments in MCoCP4. We find that the grafted peptide CP4 is the longest and most stable segment, which prefers a helical structure throughout the simulation. Furthermore, we also analyze the backbone twisting and the side-chain orientation in MCoCP4 by calculating the folding index and the orientation of the Cβ atoms in DFF. Finally, several other grafting schemes between CP4 and loop 1-5 in MCoTI-I are proposed and analyzed in a similar way.

Acknowledgements This work was supported in part by the Bulgarian National Science Fund under Grant KP-06-China-10 and KP-06-COST-9.

Computational resources were provided by the BioSim HPC Cluster at the Faculty of Physics at Sofia University "St. Kl. Ohridski", Sofia (Bulgaria) and the Centre for Advanced Computing and Data Processing, supported under Grant BG05M2OP001-1.001-0003 by the Science and Education for Smart Growth Operational Program (2014-2020) and co-financed by the European Union through the European structural and investment funds.

An Example for Application of the Simple Equaions Method (SEsM) for Obtaining Exact Solution of a Non-Linear Differential Equation with a Non-Polynomial Nonlinearity

Z. I. Dimitrova, N. K. Vitanov

We discuss the Simple Equations Method for obtaininh exact solutions of non-linear differential equations [1, 2, 3]. Recently we have shown that this method can be used also for obtaining exact solutions of classes of non-linear differential equations which contain non-polynomial non-lineairy [4]. In this presentation we demostrate the methodology by applying it step-by step to a differntail equation with a non-polynomial non-linearity. We discuss the ralationships among the parameters of the obtained exact solutions.

References

[1] Vitanov, N. K., Dimitrova, Z. I., Vitanov, K. N. (2021). Simple Equations Method (SEsM): Algorithm, Connection with Hirota Method, Inverse Scattering Transform Method, and Several Other Methods. Entropy, 23(1), 10.

[2] Vitanov, N. K., Dimitrova, Z. I. (2021). Simple equations method (SEsM) and its particular cases: Hirota method. In AIP Conference Proceedings, 2321, No. 1, 030036).

[3] Vitanov, N. K., Dimitrova, Z. I., Vitanov, K. N. (2021). On the Use of Composite Functions in the Simple Equations Method to Obtain Exact Solutions of Nonlinear Differential Equations. Computation, 9(10), 104.

[4] Vitanov, N. K., Dimitrova, Z. I. (2021). Simple Equations Method and non-linear differential equations with non-polynomial non-linearity. Entropy, 23 (12), 1624.

Reconstruction of the Initial Concentrations and the Mass Transfer Coefficient in a Model of Porous Media

T. B. Gyulov, L. G. Vulkov

A class of models in the theory of filtration in porous media are formed by systems of parabolic partial and ordinary differential equations. A simple model [1] can be reduced to the integro-differential equation:

$$\frac{\partial u}{\partial t} - \nabla.(a\nabla u - \overrightarrow{v}u) + r(x)u = f + \alpha K_s K_H \int_0^t u(x,s)ds \ \text{ in } \ Q_T, \tag{1}$$

subject to the boundary and initial conditions:

$$u(x,t) = \gamma(x,t) \quad \text{on} \quad D_T, \qquad a(x)\frac{\partial u}{\partial \nu} = \mu(x,t) \quad \text{on} \ \ N_T, \tag{2}$$

$$u(x,0) = u_0(x) \quad \text{in} \quad \Omega. \tag{3}$$

Here $\Omega \subset \mathbb{R}^d$, $d = 1, 2, 3$, is a Lipschitz domain, $Q_T = \Omega \times (0,T)$, $D_T = \Gamma_1 \times (0,T)$, $N_T = \Gamma_2 \times (0,T)$ with $\Gamma_1 \cup \Gamma_2 = \partial\Omega$, $a = a(x)$ is *a uniformly positive function* and $r = r(x) = K_s(x) - \alpha K_H$, K_s is the mass transfer coefficient. In this form, we pose the **direct** problem in which the source $f = f(x)$, the coefficients of the equation, the Dirichlet and Neumann boundary conditions and the initial condition are given. The **inverse** problem is to reconstruct

$$(K_s(x), u_0(x), f(x), u(x,t)) \in L_\infty(\Omega) \times H^1(\Omega) \times L_2(\Omega) \times H^{2,1}(Q_T)$$

satisfying (1)-(3) together with the concentrations at two time instants t_1, t_2, $0 < t_1 < t_2 < T$ and at the final time T, i.e.,

$$u(x,t_1) = \phi_1(x), \ \ u(x,t_2) = \phi_2(x), \ \ u(x,T) = \phi_T(x), \ \ x \in \Omega. \tag{4}$$

Here $\phi_1(x), \phi_2(x)$ and $\varphi_T(x)$ are given data in $L_2(\Omega)$ which may be subject to noise due to measurement errors, as

$$\|\phi_1^\varepsilon - \phi_1\|_{L^2(\Omega)} \le \varepsilon, \ \ \|\phi_2^\varepsilon - \phi_2\|_{L^2(\Omega)} \le \varepsilon, \ \ \|\phi_T^\varepsilon - \phi_T\|_{L^2(\Omega)} \le \varepsilon,$$

where $\varepsilon \ge 0$ represents the noise level. We also consider a time-averaged measurement

$$\int_0^t \omega(t)u(x,t)dt = \phi(x), \ \ \text{where} \ \ \omega(t) \ \ \text{is a weight.} \tag{5}$$

There is a great deal of problems which may be formulated for the determination of the space dependent unknowns, e.g., **reconstruction of the diffusion coefficient**;

reconstruction of the mass transfer coefficient $K_s(x)$ at one of the above measurements; **reconstruction of the initial concentration $u_0(x)$**; **simultaneous reconstruction of the mass transfer coefficient at a pair of the above measurements**; **simultaneous reconstruction of the mass transfer coefficient and the source term $f(x)$ at a pair of the above measurements**; **simultaneous reconstruction of the mass transfer coefficient $K_s(x)$ initial concentration $u_0(x)$ and the source term $f(x)$ at a triple of the above measurements**.

We focus on the determination of the space-dependent mass transfer coefficient $K_s(x)$ from the final time or time-averaged measurement, i.e., the inverse problems (1)-(3) with either (4) (problem IP1) or (5) (problem IP2). Let $u(x,t;K_s(x)) \in H^{2,1}(Q_T)$ denote the solution of the direct problem given the unknown function $K_s(x)$. The input data $\phi_T(x)$ (or $\phi(x)$) and the output data $K_s(x)$ are both space-dependent for the considered inverse problems. The *quasi-solution* of the IP1 and IP2 is the respective minimizer over the admissible set $\mathcal{A} = \{K_s \in L_\infty(\Omega) : K_s(x) \geq 0, \text{ a.e. } x \in \Omega\}$ of the following least-squares objective functionals:

$$J_1(K_s) = \frac{1}{2}\|u(\cdot,T;K_s) - \phi_T^\varepsilon(x)\|^2_{L^2(\Omega)} \tag{6}$$

$$J_2(K_s) = \frac{1}{2}\left\|\int_0^T w(t)u(\cdot,T;K_s)dt - \phi^\varepsilon(x)\right\|_{L^2(\Omega)}, \tag{7}$$

where ϕ_T^ε or ϕ^ε are the **noisy** measurements. We formulate two results.

Theorem 1. *There exists a minimizer to the optimization problem* (1)-(3) *with* (6) *(or* (7)*).*

Consider the **adjoint** problem for the minimizer of the functional $J_1(K_s)$:

$$\begin{aligned}
&\frac{\partial z}{\partial t} + \nabla.(a\nabla z) + \overrightarrow{v}.\nabla z + (K_s - \alpha K_H)z - \alpha K_s K_H \int_0^t z(x,s)ds \\
&\qquad = -2(u(x,T;K_s) - \phi_T^2(x))\delta(t-T), (x,t) \in Q_T \\
&z = 0, \ \ (x,t) \in Q_T, \quad \frac{\partial z}{\partial \nu} = 0, \ \ (x,t) \in N_T, \quad z(x,T) = 0, \ \ x \in \Omega,
\end{aligned}$$

where δ is the Dirac delta function.

Theorem 2. *The functional $J_1(K_s)$ in* (6) *is Frechet differentiable and its gradient is*

$$J_1'(K_s) = -\int_0^T u(x,t)z(x,t)dt, \ \ \textit{where } z \textit{ satisfies the adjoint problem.}$$

The conjugate gradient method is developed and similar results about $J_2(K_s)$ are obtained

Acknowledgements This research is supported by the Bulgarian National Science Fund under the Bilateral Project KP/Russia 06/12 "Numerical methods and algorithms in the theory and applications of classical hydrodynamics and multiphase fluids in porous media" from 2020.

References

[1] Armstrong J.E., Frind G.O., Mc Ckllan R.D.: Nonequilibrium mass transfer between the vapor, aqueous and solid phases in unsutarated soils during vapor extraction water. Resources Research. **30**(2), 355-368 (1994).

Recent Advances in Rational Approximation Methods for Fractional Diffusion

C. Hofreither

Fractional calculus has recently seen a surge in interest in the applied mathematical community as a tool for modeling such disparate phenomena as subdiffusion, elastoplasticity, and for image processing. In particular, this had led to increased interest in more efficient numerical methods for solving partial differential equations involving fractional derivatives.

After a short introduction to fractional diffusion equations, we discuss how methods of rational approximation can be used to construct fast numerical solvers for such problems, initially suggested in [6]: in fact, many disparate numerical approaches can be cast into a unified rational approximation framework [7]. An analytical error bound based on this observation suggests that best uniform rational approximations of fractional power functions over the spectral interval should yield highly accurate methods.

This leads naturally to the question of how to rapidly and accurately compute such best rational approximations. We discuss the recently proposed BRASIL algorithm (Best Rational Approximation by Successive Interval Length adjustments) [8], a fixed point iteration which makes use of the so-called barycentric formula for rational interpolation and iteratively rescales the intervals between the interpolation node in order to equilibrate the error. The method computes best rational approximations rapidly and stably, using only standard IEEE double precision arithmetic. Experiments demonstrate that it significantly outperforms previous state-of-the-art algorithms in several examples.

Going beyond direct rational approximation, in joint work with T. Danczul we establish an equivalence between two classes of methods for solving fractional diffusion problems, namely, Reduced Basis Methods (RBM) and Rational Krylov Methods (RKM) [2]. In particular, several recently proposed RBMs for fractional diffusion, namely those by Danczul and Schöberl [4], by Bonito et al. [1], and by Dinh et al. [5], can be interpreted as RKMs. This changed point of view has allowed us to give convergence proofs for some methods that did not have such a proof previously. We also propose a RKM for fractional diffusion problems with poles chosen using the best rational approximation of the function x^{-s} in the spectral interval of the spatial discretization matrix. This method is competitive with or superior to many methods from the reduced basis, rational Krylov, and direct rational approximation classes.

In more recent work jointly with T. Danczul and J. Schöberl [3], we have further extended this framework of rational Krylov methods to also apply to problems which are fractional both in time and in space. Here, rational approximations of the Mittag-

Leffler function come into play. Making use of the theory of Stieltjes and complete Bernstein functions, we obtain robust and efficient rational Krylov methods based on poles obtained from the solution of Zolotarëv's minimal deviation problem.

Finally, inspired by recent efforts of the group of S. Margenov to obtain more efficient rational approximation methods by truncating certain poles, we discuss ongoing work with I. Georgieva on the construction of a novel Newton's method for best uniform rational approximation of nondiagonal type, that is, with different degree of the numerator and the denominator. The computation of nodal derivatives of barycentric interpolants is somewhat involved and requires some tools from differential geometry.

References

[1] A. Bonito, D. Guignard, and A. R. Zhang. Reduced basis approximations of the solutions to spectral fractional diffusion problems. Journal of Numerical Mathematics, 28(3):147– 160, 2020.

[2] T. Danczul and C. Hofreither. On rational Krylov and reduced basis methods for fractional diffusion. Journal of Numerical Mathematics, 2021.

[3] T. Danczul, C. Hofreither, and J. Schöberl. A unified rational Krylov method for elliptic and parabolic fractional diffusion problems. Technical Report arXiv:2103.13068, arXiv, 2021.

[4] T. Danczul and J. Schöberl. A reduced basis method for fractional diffusion operators II, 2020.

[5] H. Dinh, H. Antil, Y. Chen, E. Cherkaev, and A. Narayan. Model reduction for fractional elliptic problems using Kato's formula. arXiv:1904.09332 [math.NA], April 2019.

[6] S. Harizanov, R. Lazarov, S. Margenov, P. Marinov, and Y. Vutov. Optimal solvers for linear systems with fractional powers of sparse SPD matrices. Numerical Linear Algebra with Applications, 25(5):e2167, 2018.

[7] C. Hofreither. A unified view of some numerical methods for fractional diffusion. Computers & Mathematics with Applications, 80(2):332–350, 2020.

[8] C. Hofreither. An algorithm for best rational approximation based on barycentric rational interpolation. Numerical Algorithms, 2021.

Newton's Method for Computing Periodic Orbits of the Planar Three-Body Problem

I. Hristov, R. Hristova, I. Puzynin, T. Puzynina, Z. Sharipov, Z. Tukhliev

A breakthrough in numerical searching of periodic orbits of the planar three-body problem was made in recent years. In 2013 Shuvakov and Dmitrashinovich found 13 new topological families applying a clever numerical algorithm in the standard double precision arithmetic [1]. Since the three-body problem is very sensitive on the initial conditions, working with double precision strongly limits the number of solutions that can be found. This limitation was recognized by Li and Liao, in 2017 they applied Newton's method to find more than 600 new families of periodic orbits [2]. They formed the linear system at each step of Newton's method by solving a system of ODEs with the high order multiple precision Taylor series method. However, no details of the numerical procedure are given in [2]. This numerical procedure is rather technical and deserves its own attention. In this work we present in detail Newton's method and also its modification, based on the Continuous analog of Newton's method for computing periodic orbits of the planar three-body problem. Our programs are tested in relatively short periods. We take candidates for correction with greater than usual return proximity and correct them with the modified Newton's method. As a result we find some new topological families that are not included in the database in [2]. The computations are performed in "Nestum" cluster, Sofia, Bulgaria and "Govorun" supercomputer, Dubna, Russia.

References

[1] Shuvakov, Milovan, and Veljko Dmitrashinovich. "Three classes of Newtonian three-body planar periodic orbits." Physical review letters 110.11 (2013): 114301.

[2] Li, XiaoMing, and ShiJun Liao. "More than six hundred new families of Newtonian periodic planar collisionless three-body orbits. " SCIENCE CHINA Physics, Mechanics and Astronomy 60.12 (2017): 1-7.

Computational Homogenization and Parametric Study for Materials with Closed Voids

R. Iankov, I. Georgiev, E. Kolosova, M. Chebakov, M. Datcheva

In this work, a 3D hybrid numerical-experimental homogenization strategy is proposed for determination of elastic characteristics of materials with closed voids. The performed homogenization procedure employs experimental data from micro-computed tomography (micro-CT) and instrumented indentation testing data (IIT). The results from the micro-CT testing are used to assess basic geometrical characteristics of the considered material with voids such as the volume fractions of the voids and the solid phases, the average size of the voids, the void size distribution. Furthermore, the elastic properties of the solid phase are determined based on IIT data from testing of small volumes of the selected material with voids.

For the numerical homogenization procedure, a representative volume element (RVE) is used and the micro-CT data allow to create a 3D geometrical model of the RVE reflecting the average geometrical characteristics of the tested material with closed voids. When the numerical model of the RVE is created, the following principle of equivalence is respected: the porosity assigned to the RVE is the same as the porosity calculated based on the micro-CT images. Next, this RVE geometrical model is used to generate the corresponding finite element model where, for simplicity, the voids are considered to have a spherical form as it is depicted in Fig. 1. The employed in the homogenization constitutive model for the RVE and for the solid phase material is the linear elastic model. In order to apply the homogenization technique, in the finite element model of the created RVE of the material with voids, proper periodic boundary conditions are imposed together with unit forces applied in normal (Ox, Oy, Oz) and shear directions (Oxy, Oyz, Ozx) . The resulted within the numerical homogenization procedure six boundary value problems with periodic boundary conditions are solved using the finite element code ANSYS.

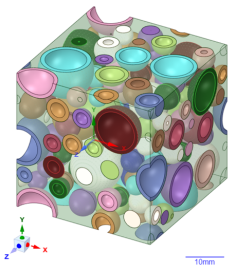

Figure 1: RVE with random particle distribution and spherical voids.

Moreover, accounting the uncertainty in the experimentally determined elastic characteristics and porosity, a parametric study was performed varying the porosity and the elastic modules within the confidence intervals of the corresponding measured values. An exaple for the elastic mudulus variation with varying the porosity is depicted in Fig. 2. The obtained results for the characteristics of the homogenized material properties are presented in a graphical form and discussed. The determined elastic characteristics are analysed against data from literature in order to reveal the applicability of the used in this study homogenization procedure.

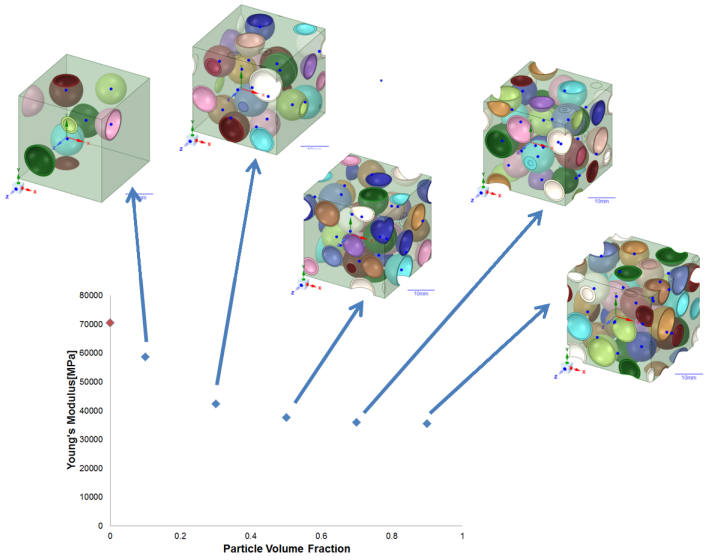

Figure 2: Parametric study results for the elastic module depending on porosity.

Acknowledgments The financial support provided by the Bulgarian National Science Fund, grants KP-06-H27/6 from 08.12.2018 (I.G.) and KP-06-Russia-1 from 27.09.2019 (M.D.&R.I.), as well as the funding by the Russian Foundation for Basic Research according to the research project No. 19-58-18011 Bulg_a (E.K.&M.Ch.) are gratefully acknowledged. We also acknowledge the provided access to the infrastructure of the Laboratory for 3D Digitalization and Microstructure Analysis and of the Laboratory for Nanostructure Characterization, financially supported by the Science and Education for Smart Growth Operational Program (2014-2020) and the European Structural and Investment fund through grants BG05M2OP001-1.001-0003 and BG05M2OP001-1.001-0008.

Numerical Validation of Analytical Solutions of Non-Stationary Wave Propagation Problems

R. Ivanov, S. Pshenichnov, M. Datcheva

The use of materials having hereditary properties in the industry is getting more and more widespread. In light of this fact, it is important to be confident about the fidelity of results obtained by numerical simulation of products made of such materials subjected to mechanical actions. A number of analytical or semi-analytical solution of generic problems of viscoelasticity are available, but their scope will never be sufficient to cover the variety and complexity of circumstances which may arise in practice. The importance of analytical solutions however lays in the fact that they can serve as reference problems by which numerical modelling techniques may be developed, calibrated and substantiated. The opposite is also true; once a theoretical solution is obtained it is desirable that it be validated by a numerical solution to eliminate a possibility for a discrepancy in the theoretical solution itself. It can be therefore said that the validation process is reciprocal.

In this study, theoretical solutions obtained by the first author were compared to solutions of the same problems obtained by the Finite Element Method (FEM), more specifically by the commercial software package ABAQUS [3]. The theoretical solutions were obtained by applying the usual in such cases Laplace transform technique with consequent inversion [1], [2]. In the course of preparing FEM input data, the relation between kernel parameters in dimensionless time used in the theoretical developments, and the Prony series expansion used in the numerical simulation of viscoelasticity in the time domain was established. Three generic problems were considered:

(a) P-wave propagation through a layer subjected to a triangular or smoothed-step normal stress pulse applied on the surface;

(b) P-wave propagation through the cross section of an infinitely long cylinder subjected to a smoothed-step normal stress pulse applied on the surface and

(c) S-wave propagation through the cross section of an infinitely long cylinder subjected to a smoothed-step shear stress pulse applied on the surface.

Several versions of viscoelastic material behavior were considered by changing the parameters of the relaxation kernels. For the layer problem, a singular relaxation kernel was considered as well.

An excellent match was achieved for the wave propagation velocities, the shape and maginitude of the stress spikes, and the apparent damping of wave motion for all cases

where regular relaxation kernels were applied, the results being practically identical. For the singular kernel however, the numerical solution resembles the analytical one only in an average sense; that is, the area of the peaks regions is practically identical, and so is the apparent damping of both the analytical and the numerical solution. The shape of the peak regions however is gently curved in the analytical solution, while in the numerical solution it is sharp and trapezoid-like.

Acknowledgement This study was performed within the bilateral project funded by the Russian Foundation for Basic Research (RFBR), project number 20-58-18002 and by the Bulgarian National Science Fund, project number KP-06-Russia/5 from 11.12.2020.

References

[1] J. Achenbach, "Vibrations of a Viscoelastic Body", AIAA Journal, vol. 5 (6), 1967, pp. 1213-1214.

[2] I. Colombaro, A. Giusti and F. Mainardi, "On the Propagation of Transient Waves in a Viscoelastic Bessel Medium", Z. Angew. Math. Phys. vol. 68, 2017, https://doi.org/10.1007/s00033-017-0808-6.

[3] Dassault Systemes Simulia Corp, ABAQUS Analysis User's Manual 6.12-13, 2012.

Solitary Travelling Waves in a Model for Spatial-Time Interaction of Populations

I. P. Jordanov

We have observed in the last decades of a fast growth of research on nonlinear phenomena. Today this is a new established research area and the research on nonlinear models finds its significant place within this area. Most nonlinear models in the research are the model patterns composed of partial differential equations (PDEs). Traveling wave solutions of these equations are of special interest as they describe the motion of wave fronts or the motion of boundary between two different states existing in this system. Unfortunately, an all encompassing method for the solution of nonlinear PDEs does not exist. Thus, nonlinear wave solutions must be sought on a case by case basis depending on the equation. In this study we study a generalized reaction-diffusion model presented, which describes spatio-temporal dynamics of interacting agents. The model describes several novel features of the interacting agents compared to the well-known classic models in population dynamics. Various analytical methods are available to find wave solutions of PDEs. In this study, we will use a particular case of the recently developed SEsM (Simple Equations Method) namely the Modified method of Simplest Equation [1, 2] and one of its extended versions [3, 4]. We will obtain a new traveling wave solution of the model system. Numerical simulations of this solution demonstrate propagation of nonlinear waves in the considered model. The characteristics of the obtained traveling wave solution are visualized and discussed.

Acknowledgments This work contains results, which are supported by the UNWE project for scientific research with grant agreement No. NID NI – 15/2020 and No. NID NI – 17/2021

References

[1] Nikolay K. Vitanov, Zlatinka I. Dimitrova, Holger Kantz. Modified method of simplest equation and its application to nonlinear PDEs. *Applied Mathematics and Computation* **216**, 2587 - 2595 (2010).

[2] Nikolay K. Vitanov. Modified method of simplest equation: Powerful tool for obtaining exact and approximate traveling-wave solutions of nonlinear PDEs. *Communications in Nonlinear Science and Numerical Simulation* **16**, 1176 - 1185 (2011).

[3] Nikolay K. Vitanov, Zlatinka I. Dimitrova, Kaloyan N. Vitanov. Modified method of simplest equation for obtaining exact analytical solutions of nonlinear partial

differential equations: further development of the methodology with applications. *Applied Mathematics and Computation* **269**, 363 - 378 (2015).

[4] Nikolay K. Vitanov, Zlatinka I. Dimitrova. Simple Equations Method and Non-Linear Differential Equations with Non-Polynomial Non-Linearity. *Entropy* **23** (12):1624 DOI:10.3390/e23121624 (2021).

Using 3D Printers for Visualization of Nonlinear Equations Solutions in the Learning Process

I. P. Jordanov, M. Georgieva, M. Ilieva, K. Damov, M. T. Iliev

Three-dimensional printing or so-called 3D printing is a state of the art technology for arbitrary shapes visualization. This method is based on a pre-developed digital model. The model is exported to a 3D printer, followed by sequential layers of material. By this way the requested object is formed. In this sense, three-dimensional printing is fundamentally different from traditional techniques in which material is usually removed to form the requested object. We model the spatial and temporal dynamics of economic agents by a system of nonlinear partial parabolic differential equations. Depending on the nature of the system, the agents may have a variety of properties, as well as to interact in a different way. In this paper we demonstrate the capabilities of 3D printers to for visualization of solutions of non-linear parabolic equations, applicable in the economy.

Acknowledgments. This work contains results, which are supported by the: UNWE project for scientific researchers with grant agreement No. NID NI - 15/2020 and BAS – Institute of Neurobiology project FNI-3028/KP-06-PM43/6/22.12.2020

Simultaneous Numerical Reconstruction of Time-dependent Convection Coefficient and Source in Magnetohydrodynamics Flow System

J. D. Kandilarov, L. G. Vulkov

We consider a simplified MHD Hartman flow with characteristic of incompressible and Newtonian (constant viscosity) in 1-D space and the case in which the fluid flows between two parallel solid plates and the velocity in perpendicular to the magnetic vector. Moreover, the pressure in the channel is supposed to be constant and the unit vectors of the velocity, the mathematical model of describing this 1-D MHD flow system can be derived from the viscous incompressible MHD equations, which can be formulated as the following form [1]:

$$\frac{\partial u}{\partial t} - \nu \frac{\partial^2 u}{\partial x^2} = \beta(t)\frac{\partial B}{\partial x} - f(t), \tag{1}$$

$$\frac{\partial B}{\partial t} - \nu_m \frac{\partial^2 B}{\partial x^2} = \beta(t)\frac{\partial u}{\partial x}, \tag{2}$$

where the spatial variable x and the time variable t belong to the set $(x,t) \in Q_T = \Omega \times (O,T)$, $\Omega = (0,X)$; $u(x,t)$ denotes the flow velocity, $B(x,t)$ is the magnetic field, $f(t)$ is the pressure difference per unit of the channel length; the function $\beta(t)$ is a given function of the induction of the extended magnetic field and can be considered as the control input for the MHD flow; ν and ν_m are two coefficients which are related with the Reynolds number of the flow. The boundary conditions for system (1)-(2) are given as follows:

$$u(0,t) = u_l(t), \;\; u(X,t) = u_r(t), \quad B(0,t) = B_l(t), \;\; B(X,t) = B_r(t). \tag{3}$$

Furthermore, the initial conditions are given by

$$u(x,0) = u_0(x), \;\; B(x,0) = B_0(x). \tag{4}$$

In the form (1)-(4), we pose the **direct problem** in which $f(t)$, the coefficients, the boundary and the initial conditions are given. Consider the **inverse** problem in which the coefficient $\beta(t)$ and the source term $f(t)$ are *unknowns*. The *additional* conditions are often stated in the form

$$\int_\Omega u(x,t)w(x)dx = \varphi(t), \;\; \int_\Omega B(x,t)\eta(x)dx = \psi(t), \tag{5}$$

where $w(x)$ and $\eta(x)$ are some weight functions. In particular, if some of these functions are Dirac-Delta functions $w(x) = \delta(x - x_*)$, $\eta(x) = \delta(x - x^*)$, $(x_*,\ x^*) \in \Omega$, then the conditions (5) take the form

$$u(x_*,t) = \varphi(t), \quad B(x^*,t) = \psi(t). \tag{6}$$

We assume that inverse problem of finding $\{u(x,y,t),\ B(x,y,t),\ \beta(t),\ f(t)\}$ has a unique solution. It is nonlinear and we use a special decomposition for which the transition to the new time level is carried out by solving three systems of boundary value problems. To implement the Rothe's method we define the time grid $\overline{\omega}_\tau = \omega_\tau \cup \{T\} = \{t^n = n\tau,\ n = 0, ..., N,\ \tau N = T\}$. We approximate the system (1)-(2) on the new time level:

$$\frac{u^{n+1}-u^n}{\tau} - \frac{1}{2}\nu\left(\frac{\partial^2 u^{n+1}}{\partial x^2} + \frac{\partial^2 u^n}{\partial x^2}\right) = \beta^{n+1/2}\frac{\partial B^{n+1/2}}{\partial x} - \frac{1}{2}\left(f^{n+1}+f^n\right) \quad (7)$$

$$\frac{B^{n+1}-B^n}{\tau} - \frac{1}{2}\nu_m\left(\frac{\partial^2 B^{n+1}}{\partial x^2} + \frac{\partial^2 B^n}{\partial x^2}\right) = \beta^{n+1/2}\frac{\partial u^{n+1/2}}{\partial x}. \quad (8)$$

The linearization is based on the approximation to the expression $p(t)q(t)$ at $t = t^{n+1/2}$: $p(t^{n+1/2})q(t^{n+1/2}) = (p(t^{n+1})q(t^n) + p(t^n)q(t^{n+1}))/2 + O(\tau^2)$. Then we use the *decompositions*

$$u^{n+1(x)} = a^{n+1}(x) + \beta^{n+1}b^{n+1}(x) + f^{n+1}c^{n+1}(x), \quad (9)$$

$$B^{n+1}(x) = d^{n+1}(x) + \beta^{n+1}e^{n+1}(x) + f^{n+1}g^{n+1}(x) \quad (10)$$

to obtain three systems of ODEs:

$$\frac{a^{n+1}-u^n}{\tau} - \frac{1}{2}\nu\frac{d^2a^{n+1}}{dx^2} - \frac{1}{2}\beta^n\frac{dd^{n+1}}{dx} = \frac{1}{2}\nu\frac{d^2u^n}{dx^2} - \frac{1}{2}f^n, \quad (11)$$

$$\frac{d^{n+1}-B^n}{\tau} - \frac{1}{2}\nu_m\frac{d^2d^{n+1}}{dx^2} - \frac{1}{2}\beta^n\frac{da^{n+1}}{dx} = \frac{1}{2}\nu_m\frac{d^2B^n}{dx^2},$$

$$\frac{b^{n+1}}{\tau} - \frac{1}{2}\nu\frac{d^2b^{n+1}}{dx^2} - \frac{1}{2}\beta^n\frac{de^{n+1}}{dx} = \frac{1}{2}\frac{dB^n}{dx}, \quad (12)$$

$$\frac{e^{n+1}}{\tau} - \frac{1}{2}\nu_m\frac{d^2e^{n+1}}{dx^2} - \frac{1}{2}\beta^n\frac{db^{n+1}}{dx} = \frac{1}{2}\frac{du^n}{dx},$$

$$\frac{c^{n+1}}{\tau} - \frac{1}{2}\nu\frac{d^2c^{n+1}}{dx^2} - \frac{1}{2}\beta^n\frac{dg^{n+1}}{dx} = -\frac{1}{2}, \quad (13)$$

$$\frac{g^{n+1}}{\tau} - \frac{1}{2}\nu_m\frac{d^2g^{n+1}}{dx^2} - \frac{1}{2}\beta^n\frac{dc^{n+1}}{dx} = 0,$$

equipped with proper boundary conditions. We first solve these ODEs boundary value problems for a^{n+1}, b^{n+1}, c^{n+1}, d^{n+1}, e^{n+1}, g^{n+1}. Then, using the decompositions (9)-(10) at the points $x = x_*$ $x = x^*$ and the observations (6) we obtain a system to find β^{n+1} and f^{n+1}:

$$u^{n+1}(x_*) = a^{n+1}(x_*) + \beta^{n+1}b^{n+1}(x_*) + f^{n+1}c^{n+1}(x_*) = \varphi(t^{n+1}), \quad (14)$$

$$B^{n+1}(x^*) = d^{n+1}(x^*) + \beta^{n+1}e^{n+1}(x^*) + f^{n+1}g^{n+1}(x^*) = \psi(t^{n+1}). \quad (15)$$

The approach described can be generalized to multi-dimensional space problems.

This work is supported by the Bulgarian National Science Fund under the Bilateral Project KP/Russia 06/12 "Numerical methods and algorithms in the theory and

applications of classical hydrodynamics and multiphase fluids in porous media" from 2020.

References

[1] L.D. Landav, J. Bell , M. Kearsley, L. Pitaevski, E. Lifshitz, and J. Sykes, Electrodynamics of Continuous Media, Elsevier, 2013

An Asymptotic Theory for a Functionally Graded Plate

J. Kaplunov, B. Erbaş, N. Ege

3D dynamic equations in linear elasticity for a transversely inhomogeneous isotropic layer are analysed at the low frequency limit. The thickness of the layer is assumed to be small in comparison with a typical wave length, while Young's modulus, Poisson's ration and mass density are defined as arbitrary functions in the transverse variable. For the sake of simplicity, the case of free layer faces is considered.

The same asymptotic scaling, as in the homogeneous setup, is adapted for 3D displacements and stresses, e.g. see [1, 2]. In this case, characteristic time and length scales are related to each other as in the classical Kirchhoff theory for plate bending. As usual, all the sought for quantities are expanded in series in terms of a small geometric parameter corresponding to the relative thickness. At leading order, we arrive at a 2D fourth order equation for bending motion taking the same form as that in the Kirchhoff theory to within the expressions for constant coefficients, which are now given by certain integrals across the thickness involving variable problem parameters.

The asymmetry of the 3D original problem with respect to the transverse variable results in presence of quasi-static extension governed at leading order by 2D equations similar to those for the generalised plane stress. It is remarkable that, in spite of asymmetry, the aforementioned problem can be decoupled, i.e. the bending sub problem is solved independently from the extension one, whereas the latter is treated with terms determined from the solution of the bending sub problem in its right hand side. It is also worth noting that the adhoc engineering formulations for functionally graded plates, e.g. see, [3, 4, 5, 6] and references therein, do not assume the possibility of such decoupling leading to differential equations of a doubled order.

The next order asymptotic approximation for plate bending is also derived. The equation of motion is still of the fourth order as at the leading-order approximation, i.e. it does not support spurious solutions similar to the homogeneous setup [1]. Higher-order corrections come through a mixed fourth order time-space derivative. However, the constant coefficients in the refined 2D bending equation are expressed through rather sophisticated multiple integrals across the thickness. Nevertheless, decoupling of bending motions and extension deformations occur at higher order as well.

Any comparison with related adhoc refined plate bending does not seem to be fruitful. The point is that the asymptotic cross section thickness variation of the displacement field at higher order nontrivially depends on variable problem parameters and cannot be approximated through simple polynomials typical of many engineering assumptions. In addition, adhoc models usually deal with stress resultants and stress couples

and therefore neglect the peculiarities of the cross thickness variation of the stress field, which is of particular importance namely for functionally graded structures.

The developed asymptotic framework is also valid for layered plates with piecewise uniform problem parameters. It also allows various extensions, including analysis of functionally graded shells, coatings and interfacial layers.

References

[1] Kaplunov, J. D., Kossovitch, L. Y., Nolde, E. V. (1998) Dynamics of thin walled elastic bodies, Academic Press.

[2] Erbaş, B., Kaplunov, J., Nolde, E., & Palsü, M. (2018). Composite wave models for elastic plates. Proceedings of the Royal Society A: Mathematical, Physical and Engineering Sciences, 474(2214), 20180103.

[3] Jha, D. K., Kant, T., & Singh, R. K. (2013). A critical review of recent research on functionally graded plates. Composite Structures, 96, 833-849.

[4] Thai, H. T., & Kim, S. E. (2015). A review of theories for the modeling and analysis of functionally graded plates and shells. Composite Structures, 128, 70-86.

[5] Amirpour, M., Das, R., & Flores, E. I. S. (2017). Bending analysis of thin functionally graded plate under in-plane stiffness variations. Applied Mathematical Modelling, 44, 481-496.

[6] Reddy, J. N., Ruocco, E., Loya, J. A., & Neves, A. M. (2021). Theories and Analyses of Functionally Graded Circular Plates. Composites Part C: Open Access, 100166.

Determination of External Boundary Conditions of a Stationary Nonlinear Problem on Disjoint Intervals

M. N. Koleva, Z. D. M. Jeknić, L. G. Vulkov

We consider a mathematical model of fluid-porous interfaces in a simple channel geometry. In this paper we deal with numerical identification of the external boundary conditions for a stationary nonlinear problem on disjoint intervals. The direct(forward) mathematical problem is to find the functions $(u_1, u_2) \in H' \equiv H^1(\Omega_1) \times H^1(\Omega_2)$ which obey (in a weak sense) the ordinary differential equations (ODEs)

$$L_1 u_1 \equiv -\frac{d}{dx}\left(p_1(x)\frac{du_1}{dx}\right) = f_1(x, u_1), \quad x \in \Omega_1 = (a_1, b_1), \tag{1}$$

$$L_2 u_2 \equiv -\frac{d}{dx}\left(p_2(x)\frac{du_2}{dx}\right) = f_2(x, u_2), \quad x \in \Omega_2 = (a_2, b_2), \tag{2}$$

at external boundary conditions

$$u_1(a_1) = \varphi_1, \quad u_2(b_2) = \varphi_2, \tag{3}$$

and internal (interface) mixed-type boundary conditions

$$l_1 u_1 \equiv p_1(b_1)\frac{du_1}{dx}(b_1) = \alpha_1 u_1(b_1) + \beta_1 u_2(a_2) + \gamma_1, \tag{4}$$

$$l_2 u_2 \equiv p_2(a_2)\frac{du_2}{dx}(a_2) = \alpha_2 u_1(b_1) + \beta_2 u_2(a_2) + \gamma_2, \tag{5}$$

where $a_1 < 0$, $b_1 \leq 0$, $a_2 \geq 0$, $b_2 > 0$, $b_1 \neq a_2$ and φ_i, α_i , β_i , γ_i, $i = 1, 2$ are given constants. For example, the case of right - hand side

$$f_i(x, u_i) = K_i \sinh(u_i) + g_i(x), \quad i = 1, 2 \;\; K_i > 0 \;\text{ constants.} \tag{6}$$

the equations (1)-(6) are Poisson-Boltzmann equations and the problem models cell-foreign interaction [2]. The direct problem is concerned with the determination of the function $u_1(x)$, $u_2(x)$ in Ω_1 and Ω_2, respectively, when all the input data in (1)-(5) are given.

Consider the *inverse* problem in which the external boundary conditions (3) are unknown, i.e. the constants φ_1, φ_2 are unknown. The additional conditions we take in the form

$$\int_a^b u_1(x) w_1(x) dx = \psi_1, \quad \int_c^d u_2(x) w_2(x) dx = \psi_2, \tag{7}$$

where $w_1(x), w_2(x)$ are weighted functions. In particular, for

$$w_1(x) = \delta(x - x_1^*), \; x_1^* \in \Omega_1 \;\text{ and }\; w_2(x) = \delta(x - x_2^*), \; x_2^* \in \Omega_2,$$

where $\delta(\cdot)$ is Dirac-delta function. From conditions (7), we have point observations

$$u_1(x_1^*) = \psi_1, \;\; u_2(x_2^*) = \psi_2. \tag{8}$$

We show that at some conditions the inverse problem for finding the fourth $\{u_1(x), u_2(x), \varphi_1, \varphi_2\}$ is well posed and propose an iterative process for the forward problem. A finite difference scheme is used to realize the algorithms proposed. First, we decouple the full inverse nonlinear problem into two Dirichlet inverse problems. Then, for the linear problem, we use a decomposition technique to obtain exact formulas for the unknown boundary conditions at points and integral measurements:

$$u_1(x) = U_1(x) + u_1(a_1)W_1(x), \;\; x \in \Omega_1,$$
$$u_2(x) = U_2(x) + u_2(b_2)W_2(x), \;\; x \in \Omega_2$$

A discrete version of the analytical approach is employed for the linear problem. All these techniques are realized to the nonlinear problems by an iterative monotone process.

The solving of the inverse problem can be described by the following algorithm

Algorithm

- Input data: observations (8) and model parameters;
- Find $u_1(b_1)$ and $u_2(a_2)$, after solving the direct problem in the intervals $[x_1^*, b_1]$, $[a_2, x_2^*]$, setting Dirichlet boundary conditions $u_1(x_1^*) = \psi_1$, $u_2(x_2^*) = \psi_2$. As a result, the inverse problem is decoupled into two independent ones on Ω_1 and Ω_2, respectively;
- Find analytically or numerically U_1, W_1 and U_2, W_2;
- Determine φ_1 and φ_2 and then find analytical or numerical solution (u_1, u_2)

$$\varphi_1 = \frac{\psi_1 - U_1(x_1^*)}{W_1(x_1)}, \quad \varphi_2 = \frac{\psi_2 - U_2(x_2^*)}{W_2(x_2)}.$$

Let us note that the efficient technique for decoupling is the two-grid method [1]. Numerical examples are discussed. In a similar way can be solved the inverse problem of the unknown boundary condition $u_2(b_2) = \varphi_2$ at the observation $u_1(x_1^*) = \psi_2$. The proposed approach also works for 2D inverse problems.

References

[1] Jovanović, B., M. Koleva, Vulkov, L.:Convergence of a FEM and two-grid algorithms for elliptic problems on disjoint domains, Journal of Computational and Applied Mathematics 236 (2011) 364–374.

[2] Vulkov, L.: Well posedness and monotone iterative method for nonlinear interface problem on disjoint intervals, AIP CP 946, 188, 2007.

Interaction of hIFNγ and Heparin-Derived Oligosaccharides

E. Lilkova, N. Ilieva, P. Petkov, L. Litov

Human interferon-gamma (hIFNγ) is a crucial immunomodulating cytokine, which biological effects may range from proliferation to apoptosis. It mediates its pleiotropic effects on cells by binding to the cell-surface domain of a high-affinity receptor hIFNγR1 to form a symmetric complex. On each side of the molecule there is a complex receptor-binding interface for each receptor that encompasses the N-terminal part of one monomer, and the C-terminal helix of the other monomer. The C-terminal domain of the cytokine does not appear to directly form a contact interface with the receptor. This part of the cytokine is a highly positively charged, solvent exposed tail, lacking a rigid conformation and is highly susceptible to proteolytic processing. The length of the C-tails plays a modulating role in the affinity of hIFNγ towards its receptor.

IFNγ is known to bind to the glycosaminoglycans (GAGs) heparin and heparan sulfate (HS). These are linear negatively charged polymers of repeating disaccharide units, containing glucosamine and uronic acid, that can bear multiple N-sulfate, N-acetyl, and O-sulfate substitutions. The binding of hIFNγ to HS and heparin modulates the blood clearance, the subsequent tissue targeting, the local accumulation of the cytokine and the proteolytic processing of its C-terminal domain.

Here, we report computational studies of the interaction of hIFNγ and heparin-derived oligosaccharides in two different scenarios – in the circulation, and at the cell-surface, when the cytokine forms a complex with its receptor.

Overexpression of IFNγ is observed in a number of autoimmune diseases, and acute states, such as a cytokine storm. A possible treatment strategy consists in inhibiting the biological activity of IFNγ. Our in silico experiments show, that heparin-like oligosaccharides bind to the C-termini of IFNγ with high affinity, forming very stable complexes due to the strong electrostatic attraction. The carbohydrates also interact with the positively charged solvent-exposed domains in the cytokine globule. After binding of several oligosaccharides, the hIFNγ–heparin complex changes its net charge from positive to neutral or even negative. This impedes further interaction of the cytokine with the extracellular part of the IFNγR1 (also negatively charged) which is the first necessary step in the IFNγ transduction pathway.

On the other hand, GAGs, and HS in particular, may be crucial participants in the formation of the hIFNγ–hIFNγR complex at the cell surface. When the cytokine is at distances greater than few Å from the receptors, the activity is determined mainly by the electrostatic interaction between the positive electric charge in the cytokine C-termini and the negative one in the receptors units. In the next stage, when the

positively charged tails and the negatively charged receptors are closer and interact more intensively, the high flexibility of the C-termini prevents proper formation of the hIFNγ–IFNγR1 complex. One possibility is the interaction of the tails with another negatively charged molecule, located at the cell surface, which would attract the C-termini and allow the cytokine to adopt proper conformation. HS is appropriate candidate, since it is the second known ligand of the hIFNγ and forms proteoglycans on the cell surface. Our in silico results demonstrate, that placing heparin-derived oligosaccharides between the two receptor units at the membrane surface does indeed facilitate the formation of the cytokine–receptor complex by pulling down the hIFNγ globule via electrostatic attraction of its C-termini.

Acknowledgements This work was supported in part by the Bulgarian National Science Fund under Grant DN- 11/20/2017.

Computational resources were provided by the Centre for Advanced Computing and Data Processing, supported under Grant BG05M2OP001-1.001-0003 by the Science and Education for Smart Growth Operational Program (2014-2020) and co-financed by the European Union through the European structural and investment funds.

The Effect of the Diffusion Coefficient in a Mathematical Model of Multiple Sclerosis

A. B. Manov, T. B. Ivanov

In the present work, we consider a mathematical model of Baló's multiple sclerosis, known in the literature [1], and extend the results, known from it. The model describes the spatiotemporal evolution of three main agents, connected to the process—macrophages, cytokines, and oligodendrocytes, denoted by $\tilde{m}, \tilde{c}$ and $\tilde{d}$, respectively. The model is given with a system of three nonlinear reaction-diffusion-chemotaxis partial differential equations:

$$\frac{\partial \widetilde{m}}{\partial T} = \underbrace{\nabla \cdot (\widetilde{a}(\widetilde{m})\nabla \widetilde{m})}_{\text{Diffusion}} + \underbrace{\lambda \widetilde{m}(\bar{m} - \widetilde{m})}_{\text{Production/Decay}}$$
$$- \underbrace{\nabla \cdot (\Psi(\widetilde{m})\nabla \widetilde{c})}_{\text{Chemotaxis}}, \text{ with } \Psi(\widetilde{m}) = \chi \frac{\widetilde{m}}{\bar{m} + \widetilde{m}},$$
$$\frac{\partial \widetilde{c}}{\partial T} = \frac{1}{\nu}(\underbrace{\varepsilon \Delta \widetilde{c}}_{\text{Diffusion}} + \underbrace{\mu \widetilde{d} + b\widetilde{m}}_{\text{Production}} - \underbrace{\alpha \widetilde{c}}_{\text{Decay}}),$$
$$\frac{\partial \widetilde{d}}{\partial T} = \underbrace{\kappa F(\widetilde{m}) \widetilde{m} (\bar{d} - \widetilde{d})}_{\text{Production}}, \text{ with } F(\widetilde{m}) = \frac{\widetilde{m}}{\bar{m} + \widetilde{m}},$$

where $\widetilde{a}$ is the diffusivity of the macrophages; λ is the production rate of the activated macrophages; $\bar{m}$ is the characteristic density of macrophages, i.e., the mean value of their initial distribution in the white matter of the brain; χ is the maximum chemotattraction rate; ε is the diffusivity of the cytokines; ν is the characteristic time scale of the cytokines' rate of change; μ, b are the production rates of cytokines from destroyed oligodendrocytes and macrophages, respectively; α is the natural decay rate of cytokines; $\bar{d}$ is the initial characteristic density of oligodendrocytes in the brain, i.e., the average density of oligodendrocytes in a healthy brain; κ is the destructive strength of the macrophages.

We consider the corresponding 1D model under the assumption of radial symmetry, which is sensible for Baló's multiple sclerosis. In particular, we study how altering the diffusion coefficient affects the pattern formation of demyelinated plaques. Based on numerical experiments we first consider the effect of increasing and decreasing the constant diffusion coefficient. Then, we go on and show that introducing nonlinear diffusion coefficient might lead to quailtatively different pattern formations.

References

[1] M. Lombardo, R. Barresi, E. Bilotta, F. Gargano, P. Pantano, and M. Sammartino. Demyelination patterns in a mathematical model of multiple sclerosis. Journal of mathematical biology, 75:373–417, 2017.

Achievements and Challenges in Numerical Methods for Multidimensional Spectral Fractional Diffusion Problems

S. Margenov

Fractional diffusion operators appear naturally in various areas in mathematics, physics, ect. The most important property of the related boundary value problems is that they are nonlocal. Let us consider a fractional power of a self-adjoint elliptic operator introduced through its spectral decomposition. It is self-adjoint but nonlocal. Such problems are computationally expensive. Several different techniques were proposed during last decade to localize the nonlocal elliptic operator, thus increasing the space dimension of the original computational domain.

An alternative approach is originally proposed in [5] and further developed in [2, 3], see also the survey paper [4]. Let $\mathcal{A}$ be a properly scaled symmetric and positive definite sparse matrix, arising from finite element or finite difference discretization of the initial (standard, local) diffusion problem. Based on best uniform rational approximations (BURA) of $t^\alpha/(1+qt^\alpha)$, $q \geq$ for $t \in [0,1]$, a class of solution methods for solving algebraic systems of linear equations involving $\mathcal{A}^\alpha + q\mathcal{I}$, $0 < \alpha < 1$, is proposed and analysed. Robust error estimates with respect to the condition number $\kappa(\mathcal{A})$ are obtained, showing the exponential convergence rate of BURA methods with respect to the degree of rational approximation k. At this point we assume that some solver of optimal complexity (say multigrid or multilevel) is used for the involved systems with matrices $\mathcal{A} + d_j\mathcal{I}$, $d_j \geq 0$, $d_j \geq 0$, $j = 1, \ldots, k$. This leads at the end to an almost optimal complexity $O(N \log^2 N)$ of the algorithm. The comparative analysis demonstrates well expressed advantages of the BURA methods. A unified theoretical explanation of these observations is discussed at the end.

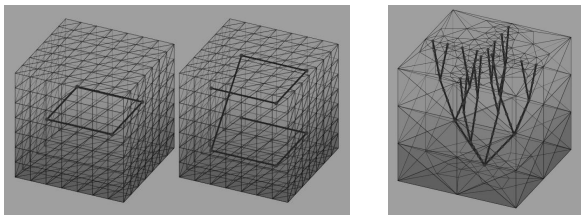

Figure 1: Fractional order preconditioning in coupled multi-scale 3D-1D problems: (a) Model problems with single line geometry of the interface(left); (b) More realistic problem with more general geometry of the interface (right)

The second part of the talk is devoted to the following challenges:

- **Low regularity and local refinement.** Some authors assume a high smoothness of the solution. However, this is far from reality. The fractional diffusion equations are less regular. Thus, the development of robust solvers for the case of adaptive local mesh refinement in is among the difficult challenges.
- **Time-dependen problems.** In some sence, solving standard parabolic problems is easier than the elliptic ones. The situation is quite different in the case of space frational time-dependent problems. It may be surprising that the matrix-vector multiplication by $\mathcal{A}^\alpha$ is a more difficult task than solving the system $\mathcal{A}^\alpha \mathbf{u} = \mathbf{f}$.
- **Coupled problems and preconditioning of fractional order operators.** The majority of real-life applications are described by coupled systems of PDEs. An example of a multi-scale time-dependent problem (see Fig. 1) is considered to illustrate some key ideas. The robust preconditioning is an important open problem.
- **Computational complexity.** The degree k is commonly accepted as an universal measure in the comparative analysis. This is not very sharp looking in the properties of the related k auxiliary linear system. This raises the question if the computational complexity can be reduced from $O(N \log^2 N)$ to $O(N \log N)$, see [2].
- **Parallel scalability.** Three levels of parallelism were implemented to prove the advantages of the BURA method in [1]. However, the real picture is substantially reacher. Balancing the parallel tasks and developing of hibrid parallel algorithms for the modern supercomputers with hibrid architecture is a key challenge for the case of extremely large-scale multiphysiscs applications.

References

[1] Coegis, R., Starikovicius, V., Margenov, S., Kriauziene, R. (2019), Scalability analysis of different parallel solvers for 3D fractional power diffusion problems, Concurrency and Computation: Practice and Experience, 31 (19), e5163, https://doi.org/10.1002/cpe.5163

[2] Harizanov, S., Kosturski, N., Lirkov, I., Margenov, S., Vutov, Y. (2021), Reduced Multiplicative (BURA-MR) and Additive (BURA-AR) Best Uniform Rational Approximation Methods and Algorithms for Fractional Elliptic Equations, Fractal and Fractional, 5 (3), 61, https://doi.org/10.3390/fractalfract5030061

[3] Harizanov, S., Lazarov, R., Margenov, S., Marinov, P., Pasciak, J. (2020), Analysis of numerical methods for spectral fractional elliptic equations based on the best uniform rational approximation, Journal of Computational Physics, 408, https://doi.org/10.1016/j.jcp.2020.109285

[4] Harizanov, S., Lazarov, R., Margenov, S., Marinov, P. (2020), A survey on numerical methods for spectral Space-Fractional diffusion problems, Fractional Calculus and Applied Analysis, 23 (6), 1605-1646

[5] Harizanov, S., Lazarov, R., Margenov, S., Marinov, P., Vutov, Y. (2018), Optimal Solvers for Linear Systems with Fractional Powers of Sparse SPD Matrices, Numerical Linear Algebra with Applications, DOI: 10.1002/nla.2167

Digital Transformation Multidimensional Security Analysis with Future Quantitative Assessment

Z. Minchev

Understanding properly the digital transformation security transcendents (like: risks, challenges, threats, opportunities, uncertainties) is a rather challenging problem especially for the future. In this context, joining human with machine beliefs and objectives solving could be a rather helpful solution [1]. Three key problems have to be outlined here: (i) the correct fusion and prioritizing of multiple dynamic information sources; (ii) successfully representing the multidimensional evolution space, using the dynamic information effectively. The (iii) resulting aggregation needs to be reasonably shown, producing a flexible classification, readjustment as neither dynamic, information sources' reliability or real dimensionality is preliminary known for the future.

The work tries to briefly present a hybrid experimentation on heuristic approach for solving the correct dimensionality of the digital transformation security multidimensional scenario modelling, and further transcendents analysis [2]. Both human future beliefs and machine scenarios smart evolution, with ad-hoc future multicriteria objectives assessment are implemented in the accomplished approach. Finally, different future findings [3] and uncertainties with the security transcendents of the digital transformation are also discussed with the outlined analytical ideas real implementation.

References

[1] Minchev, Z. Malicious Future of AI: Transcendents in the Digital Age, In Proc. of BISEC 2021, Belgrade Metropolitan University, December 3, 2021

[2] Minchev, Z., et al, Future Digital Society Resilience in the Informational Age, Sofia, SoftTrade & Institute of ICT, Bulgarian Academy of Sciences, 2019

[3] Minchev, Z., et al, Digital Transformation in the Post-Information Age, SoftTrade & Institute of ICT, Bulgarian Academy of Sciences, 2021

Implemenation, Performance and Scalability of a Large Scale Air Pollution Model on the New Eurohpc Petascale Supercomputer DISCOVERER in Bulgaria

T. Ostromsky

The environmental modelling and air pollution modelling in particular is one of the toughest problems of computational mathematics (together with the meteorological modelling). All relevant physical and chemical processes in the atmosphere should be taken into account, which are mathematically represented by a complex PDE system. To simplify it a proper splitting procedure is applied. As a result the initial system is replaced by several simpler systems (submodels), connected with the main physical and chemical processes. These systems should be calculated in a large spatial domain, as the pollutants migrate quickly on long distances, driven by the atmosphere dynamics, especially on high altitude. Here they are exposed to temperature, light and other condition changes in extremely wide range, so does the speed of most chemical reactions. One of the major sources of difficulty is the dynamics of the atmospheric processes, which require small time-step to be used (at least, for the chemistry submodel) in order to get a stable numerical solution of the corresponding system. All this makes the treatment of large-scale air pollution models a tuff and heavy computational task. It has always been a serious challenge, even for the fastest and most powerful state-of-the-art supercomputers.

The first crucial point on the way to this goal is domain decomposition technique. This is a natural way to achieve distributed memory parallelization of any numerical problem over a large spatial domain. For some of them however, like the advection-diffusion equations in our case, there is always certain overhead due to the boundary conditions. Minimizing this overhead is a key point towards efficient optimization. On the other hand, optimization should not restrict the portability of the parallel implementation, as the intensive development in the computer technology inevitably leads to regular updates or complete replacement of the outdated hardware. Standard parallel programming tools as MPI and OpenMP (for distributed / shared memory models) are used in order to preserve portability of the code. Another important parallel optimization issue is the load-balance. MPI barriers, used to force synchronization between the processes in data transfer commands, often do not allow good load-balance. This obstacle can be avoided to some extent by using non-blocking communication routines from the MPI standard library.

The basic MPI version of the Danish Eulerian Model (DEM) [5, 6] has been implemented and run on the new petascale supercomputer DISCOVERER, installed this year by Atos company at Sofia Tech Park in Bulgaria. The machine is part of the European High Performance Computing Joint Undertaking (EuroHPC). The results of preliminary scalability experiments of the basic MPI parallel implementation of DEM

on a relatively small set of nodes and with just automatic compiler-level optimizations are presented in the talk. They are compared with similar earlier experiments performed on the Mare Nostrum III supercomputer (petascale too) at Barcelona Supercomputing Centre – the most powerful supercomputer in Spain by that time, upgraded currently to the pre-exascale Mare Nostrum V, also part of the EuroHPC JC infrastructure.

DEM is a powerful and sophisticated large scale air pollution model, with some 30-year development history [1, 2, 6, 7]. Over the years it was successfully applied in different long-term environmental studies in various areas. Parallelization is primarily based on the space domain partitioning [3, 4, 6, 7].

Times (T) in seconds and speed-ups *(Sp)* for running DEM (the basic MPI version) on the EuroHPC supercomputer DISCOVERER (in Sofia Tech Park) are given in the table below.

NP	# NODES	Advection		Chemistry		TOTAL		
		T [s]	*(Sp)*	T [s]	*(Sp)*	T [s]	*(Sp)*	*E* [%]
4	1	23408	*(4.0)*	20825	*(4.0)*	48604	*(4.0)*	100 %
8	1	11830	*(7.9)*	11072	*(7.5)*	25045	*(7.8)*	97 %
12	1	7785	*(12.0)*	7112	*(11.7)*	17036	*(11.4)*	95 %
16	1	6023	*(15.5)*	5438	*(15.3)*	13061	*(14.9)*	93 %
24	2	4075	*(23.0)*	3630	*(22.9)*	9148	*(21.3)*	89 %
36	3	2786	*(33.6)*	2314	*(36.0)*	6248	*(31.1)*	86 %
60	4	1790	*(52.3)*	1358	*(61.3)*	3638	*(53.4)*	89 %
80	5	1420	*(65.9)*	978	*(85.2)*	3050	*(63.7)*	80 %
120	8	1072	*(87.3)*	662	*(125.8)*	2394	*(81.2)*	68 %
160	10	895	*(104.6)*	498	*(167.3)*	2052	*(94.7)*	59 %

Acknowledgments This research was supported in part by the Bulgarian NSF project "Efficient methods for modelling, optimization and decision making" (contract # KP-06-N52/5), and by the PetaSC - Bulgaria consortium.

References

[1] V. Alexandrov, A. Sameh, Y. Siddique and Z. Zlatev, Numerical integration of chemical ODE problems arising in air pollution models, Env. Modeling and Assessment, 2 (1997) 365–377.

[2] Ø. Hov, Z. Zlatev, R. Berkowicz, A. Eliassen and L. P. Prahm, Comparison of numerical techniques for use in air pollution models with non-linear chemical reactions, Atmospheric Environment 23 (1988), pp. 967–983.

[3] Tz. Ostromsky, Z. Zlatev, Parallel Implementation of a Large-scale 3-D Air Pollution Model, Large Scale Scientific Computing (S. Margenov, J. Wasniewski, P. Yalamov, Eds.), LNCS-2179, Springer, 2001, pp. 309–316.
[4] Tz. Ostromsky, Z. Zlatev, Flexible Two-level Parallel Implementations of a Large Air Pollution Model, Numerical Methods and Applications (I.Dimov, I.Lirkov, S. Margenov, Z. Zlatev - eds.), LNCS-2542, Springer (2002), pp. 545–554.
[5] WEB-site of the Danish Eulerian Model, available at: *http://www.dmu.dk/AtmosphericEnvironment/DEM*
[6] Z. Zlatev, Computer treatment of large air pollution models, Kluwer (1995).
[7] Z. Zlatev, I. Dimov, Computational and Numerical Challenges in Environmental Modelling, Elsevier, Amsterdam (2006).

Classification of Images for Reverse Engineering of Slot Machines

D. Parvanov, G. Mateeva, T. Balabanov

Introduction Slot machines are the most popular gambling games. Reels with drawn symbols spin on the screen. When the reels stop, the winning combinations are formed according to predefined patterns. Symbols placement in the reels is a discrete probability distribution. According to this distribution, the parameters of the game are determined. The most important parameters are - return to player and volatility. Return to player is controlled by the government authorities. Volatility shows how often and how big the wins will be. The distribution of the symbols is unknown to the player. Reverse engineering is one of the approaches to its discovery.

Reverse Engineering Slot machine screen is organized in virtual reels. Since reels are not known, the only approach to reconstructing drums is by observing chunks of them [1,2]. Approximated reconstruction is possible when chunks are strictly tagged. Tagging is a process of transforming symbols' images into exact numbers. With enough chunks of reels, reconstruction is a problem for solving a linear puzzle. The quality criterion is the achievement of the desired return to the player and variability, even when the reels are not exactly reconstructed.

Classification of Images Image classification starts by obtaining manual screenshots on the game screens. The exact areas of the locations of the symbols are given manually into the screen capture tool. The image processing software library is involved in the classification. The images are separated into classes based on a difference threshold. The main difficulties in classification come from the fact that not all symbols are pure images. Some of the symbols are included in the animations, mainly when there is prize on the screen.

Conclusions Automated classification of images has real applicability in real-life industrial analysis of slot machine gambling games. The most time-consuming part of reverse engineering in the problem described is tagging of the symbols.

Acknowledgments This research is funded by Velbazhd Software LLC and it is partially supported by the Bulgarian Ministry of Education and Science (contract D01–205/23.11.2018) under the National Scientific Program "Information and Communication Technologies for a Single Digital Market in Science, Education and Security (ICTinSES)", approved by DCM # 577/17.08.2018.

References

[1] Petrov, P., Kostadinov, G., Zhivkov, P., Velichkova, V., Balabanov, T.: Approximated Sequences Reconstruction with Genetic Algorithms, Proceedings of 28th Symposium with International Participation - Control of Energy, Industrial and Ecological Systems, 63–66, 2020.

[2] Petrov, P., Kostadinov, G., Zhivkov, P., Velichkova, V., Balabanov, T.: Approximate Sequencing of Virtual Reels with Genetic Algorithms, Proceedings of the 23rd International Conference on Distributed Computer and Communication Networks: Control, Computation, Communications, 507–514, 2020.

Nano Computing in Bioinspired Systems

A. Slavova, V. Ignatov

Information processing in the brain takes place in a dense network of neurons connected through synapses. The collaborative work between these two components (Synapses and Neurons) allows basic brain functions such as learning and memorization. An efficient emulation of these computational concepts is possible only overcoming the so call von Neumann bottleneck which limits the information processing capability of conventional systems. To this end, the mimicking the neuronal architectures with silicon-based circuits, on which neuromorphic engineering is based on, is accompanied by the development of new devices with neuromorphic functionalities.

In this talk we shall study Hodgkin–Huxley equations [1] of the cardiac Purkinje fibre (CPF) model of morphogenesis which describes the long-lasting action and pacemaker potentials of the Purkinje fibre of the heart. The FitzHugh Nagumo equation [2,3], which is a simplification of the Hodgkin-Huxley model, describes the generation and propagation of the nerve impulse along the giant axon of the squid. For dynamical systems in neuroscience, the type of bifurcation determines the computational properties of neurons. Based on the finite propagating speed in the signal transmission between the neurons, we shall derive various neural systems and study their dynamics.

We shall use concepts from nonlinear system theory to derive model representations of the mathematical description of the physical structure for analytical treatment and time efficient simulations. We then plan to investigate the dynamics of the model representations taking the stochastic variability in its nonlinear behaviour into account. It is a further goal of our experiments to reduce this variability to a suitable low level as required by the application under investigation through the optimization of the device structure and material choice. Finally, the outcome of the experimental and theoretical investigations shall support the design and fabrication of electrical circuits chosen from two distinct applications - spatio-temporal pattern recognition and digital logic - and based upon the locally-active threshold switching behaviour of our device.

Based on the local activity of cells [4], analytical criteria for computer simulations with four state variables and one diffusion coefficient will be presented. The criteria can be easily implemented by a computer program to produce bifurcation diagrams for the corresponding Hodgkin–Huxley model. Although no chaotic phenomenon is observed, the cell parameters which cause the heart to stop beating are always located near the edge of chaos domains.

References

[1] A. L. Hodgkin and A. F. Huxley, "A quantitative description of membrane current and its application to conduction and excitation in nerve," J. Physiology, vol. 117 (1952): 500–544.

[2] R. FitzHugh, "Impulses and physiological states in theoretical models of nerve membrane," Biophysics. J. 1 (1961): 445–466.

[3] J. Nagumo, S. Arimoto and S. Yoshizawa, "An active pulse transmission line simulating nerve axon," Proc. IRE 50, (1962): 2061–2070.

[4] A. Slavova, P.Zecca, Modelling Natural Phenomena via Cellular Nonlinear Networks, Cambridge Scholars Publisher, 2017.

Charge-Dependence of the Membrane Destruction Modes of Linear Antimicrobial Peptides: a Case Study

P. Petkov, N. Ilieva, E. Lilkova, L. Litov

AMPs have broad-spectrum activity against a wide variety of pathogens, including gram-positive and gram-negative bacteria, fungi, parasites, and even some viruses. They exert their action by interacting with target cellular membranes, whereas they either insert into or penetrate the lipid bilayer. It is widely accepted that the mechanism of action of AMPs is based on their cationic and amphiphilic nature, which enables them to interact with negatively charged bacterial surfaces and membranes, thus causing membrane disruption or altering metabolic processes. Therefore, understanding of the AMP's mechanism of action requires experimental studies and computational modelling of the peptide-membrane interaction. However, this interaction presents some challenges to standard atomistic simulations, due to slow relaxation times of the lipid bilayer, conformational changes in the peptides upon interaction with the membrane, peptide self-assembly and pore formation, requiring prohibitively long simulation times.

Here, we report the computational study of the interaction of a particular putative AMP with a model bacterial membrane. The studied AMP was isolated from the mucus of garden snails Helix aspersa. The model membrane is constructed to resemble the E. Coli membrane: asymmetric, with POPE (neutral) and POPG (negatively charged) phospholipids in ratios 85/15 and 70/30 in the external, resp. internal layer. To enhance the conformation space sampling of the AMP–membrane complex we employed well-tempered metadynamics, which allowed for exploration of multidimensional free energy surfaces in terms of appropriate collective variables. We demonstrate, that there are well defined minima in the free energy landscape of the interaction of the peptide and the lipid bilayer, that are dependant on the charge of the attacking peptide segment.

Acknowledgements This work was supported in part by the Bulgarian Science Fund (Grant KP-06-OPR 03-10/2018) and by the Bulgarian Ministry of Education and Science (contract DO1-358/17.12.2020) under the National Scientific Program "Innovative Low-Toxic Bioactive Systems for Precision Medicine (BioActiveMed)" approved by DCM # 658/14.09.2018.

Computational resources were provided by the BioSim HPC Cluster at the Faculty of Physics at Sofia University "St. Kl. Ohridski", Sofia (Bulgaria) and by CI TASK (Centre of Informatics – Tricity Academic Supercomputer & networK), Gdansk (Poland).

Extreme Learning DANFA Model for Electricity Consumption Prediction

M. Terziyska, K. Yotov, E. Hadzhikolev, Zh. Terziyski, S. Hadzhikoleva

Electricity consumption is an important indicator of the living standard of the population and the efficiency of economic activities. In recent years, there has been a steady increase in electricity consumption worldwide. In general, this is due to population growth, a higher level of personal comfort for people (larger homes, new and larger appliances and equipment, new services [*1*]), and economic growth in all sectors. All this shows that the management of energy demand is very important. Effective energy management is essential for economic success, environmental preservation, and suitable planning of existing resources [*2*]. Therefore, various techniques have been used for energy demand management to forecast future energy demands accurately [*3*]. Along with the well-known autoregressive models (such as ARIMA, SARIMA), data-driven machine learning algorithms such as fuzzy logic, genetic algorithm, neural network and support vector regression models are increasingly used for forecasting of the national and regional energy demand. A neural network model for long-term energy consumption prediction in Greece is presented in [*4*]. To develop this model, the authors tested ten different neural architectures. This shows the main problem with the use of neural networks, namely the lack of a unified theory to regulate the determination of the number of hidden layers and the number of neurons in them. In addition, neural networks have a large number of parameters (weights) that must be determined in the course of their training, and then this task might require high computational power. It is proven that fuzzy logic gives good results to deal with a high level of uncertainty in data. Therefore, in [*5*], [*6*] fuzzy models for electricity consumption prediction respectively in Jordan and in Brazil are proposed. The hybrid neuro-fuzzy structures are also used for energy demand forecasting [*7*], [*8*]. The Extreme Learning Distributed Adaptive Neuro-Fuzzy Architecture (ELDANFA) model, which is a modification of ANFIS is presented in this paper. The main goal for the development of such a model is to obtain an accurate model that works with minimal error and reduced computational load. The proposed model was tested by forecasting the consumed electricity in Stanimaka substation, Asenovgrad, Bulgaria. The results show that the set goals have been achieved. On one hand, the number of fuzzy rules is reduced, which makes the model suitable for real-time operation, and on the other hand, the predicted error is very small.

Acknowledgment The work is partially funded by the MU21-FMI-004 project at the Research Fund of the University of Plovdiv "Paisii Hilendarski".

References

[1] Tzeiranaki, T., Bertoldi, P., Diluiso, F., Castellazzi, L. et al.: Analysis of the EU residential energy consumption: Trends and determinants, Energies 12, no. 6 (2019): 1065.

[2] Sasan, B., Sadegh, S.: Forecasting energy consumption using ensemble ARIMA–ANFIS hybrid algorithm, International Journal of Electrical Power and Energy Systems, 82 (2016): 92-104.

[3] Suganthi, L., Samuel, AA.: Energy models for demand forecasting—a review, Renew Sustain Energy Rev, (2012) 16:1223–40.

[4] Ekonomou, L.: Greek long-term energy consumption prediction using artificial neural networks, Energy 35, no. 2 (2010): 512-517.

[5] Rustum, M., Badran, O., Abdulhadi, E.: A fuzzy inference model for short-term load forecasting, Energy Policy 37, no. 4 (2009): 1239-1248.

[6] Torrini, F., Souza, R., Oliveira, F., Pessanha, J.: Long term electricity consumption forecast in Brazil: a fuzzy logic approach, Socio-Economic Planning Sciences, 54 (2016): 18-27.

[7] Akdemir, B., Çetinkaya, N.: Long-term load forecasting based on adaptive neural fuzzy inference system using real energy data, Energy Proc. (2012) 14:794–9.

[8] Al-Ghandoor, A., Samhouri, M., Al-Hinti, I., Jaber, J., Al-Rawashdeh, M.: Projection of future transport energy demand of Jordan using adaptive neuro-fuzzy technique, Energy (2012) 38:128–35.

A Comparative Study of Methods for Scattered Data Interpolation using Minimum Norm Networks and Quartic Triangular Bézier Surfaces

K. Vlachkova, K. Radev

Scattered data interpolation is an important problem in approximation theory and geometric modeling and has numerous applications in practice. The problem can be formulated as follows: Given a set of points $(x_i, y_i, z_i) \in \mathbb{R}^3$, $i = 1, \ldots, n$, find a bivariate function $F(x, y)$ defined in a certain domain containing points $V_i = (x_i, y_i)$, such that F possesses continuous partial derivatives $\partial F/\partial x$, $\partial F/\partial y$, and $F(x_i, y_i) = z_i$.

Nielson [1] proposed a solution to the problem as follows. First, he constructed a smooth interpolation curve network with minimum L_2-norm of the second derivative (MNN) defined on the edges of an associated triangulation T. The MNN is a cubic curve network. Then he extended the MNN to a smooth rational surface using a blending method. Andersson et al. [2] gave a new proof of Nielson's result which allows them to consider and handle the case where the data are convex and a minimum L_2-norm network which is convex on the edges of T is sought. Vlachkova [3, 4] extended the results in [2] to minimum L_p-norm networks for $1 < p < \infty$. In [5] the MNN was degree elevated to quartic and an algorithm for its extension to a smooth surface consisting of quartic triangular Bézier patches was proposed.

Here we consider the following two curve networks: (i) the edge convex cubic MNN which is degree elevated to quartic; (ii) the edge convex minimum L_p-norm network for $p = 3/2$ which is slightly modified to quartic. Using the algorithm proposed in [5], we construct the corresponding two interpolation surfaces consisting of quartic triangular Bézier patches. Our goal is to evaluate and compare the quality and the shape of these surfaces. We performed a large number of experiments using data of increasing complexity and analysed the results with respect to different criteria. Here we present the results of our numerical experiments.

Example 1. The data are $(-1/2, -\sqrt{3}/6, 0)$, $(1/2, -\sqrt{3}/6, 0)$, $(0, \sqrt{3}/3, 0)$, $(0, 0, -1/2)$. The triangulation and the corresponding edge convex MNN are shown in Fig. 1. The highlight lines on the surface and the gaussian curvature are visualized in Fig. 2.

Acknowledgments This work was supported in part by European Regional Development Fund and the Operational Program "Science and Education for Smart Growth" under contract № BG05M2OP001-1.001-0004 (2018-2023).

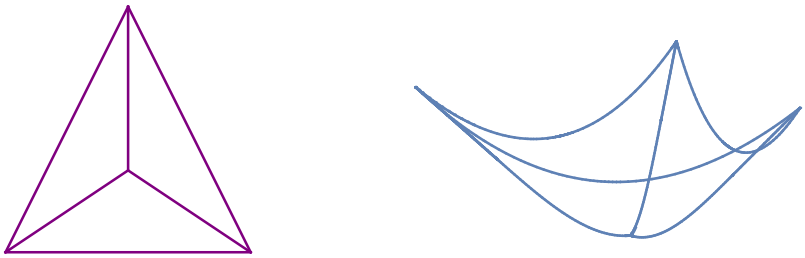

Figure 1: The triangulation and the corresponding edge convex MNN for the data in Example 1.

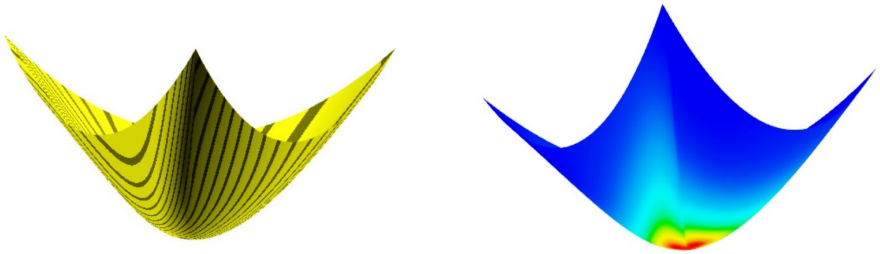

Figure 2: The surface interpolating the modified edge convex MNN for the data in Example 1: (left) Highlight lines on the surface; (right) Gaussian curvature: the color scale goes from blue (low) to red (large)

References

[1] G. M. Nielson. A method for interpolating scattered data based upon a minimum norm network. *Math. Comp.*, 40(161), 253-271, 1983. https://doi.org/10.1090/S0025-5718-1983-0679444-7

[2] L.-E. Andersson, T. Elfving, G. Iliev, K. Vlachkova. Interpolation of convex scattered data in $\mathbb{R}^3$ based upon an edge convex minimum norm network. *J. Approx. Theory*, 80(3), 299-320, 1995. https://doi.org/10.1006/jath.1995.1020

[3] K. Vlachkova, Interpolation of scattered data in $\mathbb{R}^3$ using minimum L_p-norm networks, $1 < p < \infty$, *J. Math. Anal. Appl.*, 482, 123824, 2020. https://doi.org/10.1016/j.jmaa.2019.123824

[4] K. Vlachkova, Interpolation of convex scattered data in $\mathbb{R}^3$ using edge convex minimum L^p-norm networks, $1 < p < \infty$, *AIP Conf. Proc.*, 2183, 070028, 2019. https://doi.org/10.1063/1.5136190

[5] K. Vlachkova, K. Radev, Interpolation of data in $\mathbb{R}^3$ using quartic triangular Bézier surfaces, *AIP Conf. Proc.*, 2325, 020061, 2021. https://doi.org/10.1063/5.0040457

[6] BezierView, https://www.cise.ufl.edu/research/SurfLab/bview/

Numerical Simulations of the Process of Adsorption onto Activated Carbon in Water Treatment Applications

M. N. Zarcheva, T. B. Ivanov

The present work is concerned with modelling water treatment using activated carbon filters—a widely used technology, whose proper management is essential for its effectiveness.

Activated carbon is a highly porous medium, which makes it very suitable for removing variety of pollutants from water and wastewater through the physical process of adsorption. We are interested in a particular type of activated carbon filters—granular activated carbon (GAC) column filters, in which tiny carbon particles are loosely arranged in a column. We consider a 1D setting of the process, assuming that water flows from the top ($x = X$) to the bottom ($x = 0$) of the filter at a constant rate (Figure 1). During the purification process, the liquid passes through the porous structure of the AC particles, which allows the pollutants dissolved in it to be attracted to the internal surface of the porous medium.

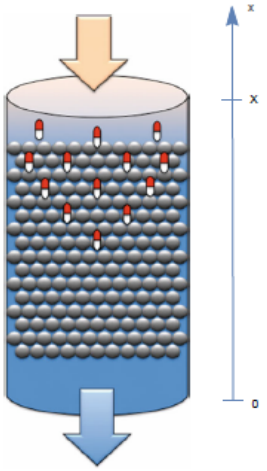

Figure 1: Inlet and outlet of a GAC filter.

The process of water purification with activated carbon can be described using a system of $2N$ non-linear partial differential equations, where N is the number of

contaminants in the water. Each contaminant can be characterized by two main quantities:

- c_i, $i = 1, \ldots, N$—the concentration of the i-th contaminant in the water;
- q_i, $i = 1, \ldots, N$—the amount of the i-th contaminant inside the carbon particles.

There are three main processes that underlie water treatment with activated carbon—advection, diffusion and adsorption. If one assumes that the adsorption is the rate-limiting process and diffusion is negligible with respect to advection, the following advection-adsorption model can be formulated:

$$\begin{aligned} \frac{\partial c_i}{\partial t} &= \frac{\nu}{\epsilon}\frac{\partial c_i}{\partial x} - \rho\frac{1-\epsilon}{\epsilon}\gamma(Q_i - q_i), \\ \frac{\partial q_i}{\partial t} &= \gamma(Q_i - q_i). \end{aligned} \tag{1}$$

The physical meaning of the given quantities is as follows: ν is the constant velocity of the water flow; ϵ is the porosity of the filter bed (the fraction of voids volume over the total body volume); $\gamma = \frac{6 \cdot 10 \cdot D_s}{d_p^2}$ is the rate of transfer of a compound from the outer surface of the particle to its interior, where D_s is the intraparticle diffusion coefficient and d_p is the activated carbon particle diameter; ρ is the density of carbon; Q_i is a nonlinear term that describes the load of compound i on the surface of the carbon particle and it depends on the adsorption properties of each particular contaminant—we use a generalization of the Freundlich isotherm with a simplified ideal adsorbed solution (SIAS) model [1].

In a recent ESGI [2], however, the numerical solution of this model was identified as a problem for various values of the model parameters. We propose a novel semi-implict scheme that allows for the efficient solution of the differential problem. The robustness of the scheme is validated for a wide range of model parameters, expected to appear in practice. The proposed numerical scheme is successfully applied to the solution of the system of 20 PDEs, corresponding to 10 different contaminants in the water. We also study numerically the rate of convergence of the scheme and the computational efficiency of the implemented algorithms for various numbers of contaminants in the water.

One of the main reasons for simulating the process is the prediction of the time when a particular carbon filter will get exhausted and needs to be replaced. Thus, we compute the so-called breakthrough curves that give information about the quality of the water treatment (i.e., how much of the pollutant is still present in the water after passing through the filter).

The numerical experiments conducted with the proposed scheme appear to reflect very well the qualitative behaviour of the process of adsorption of natural organic matter and nine different micro-pollutants onto activated carbon.

References

[1] F.A. DiGiano, G. Baldauf, B. Frick, H. Sontheimer, Simplifying the description of competitive adsorption for practical application in water treatment, Activated Carbon Adsorption of Organics from the Aqueous Phase 1 (1980) 213–228.

[2] Proceedings of the 148^{th} European Study Group
ISBN:978-94-6395-192-0.

Part B

List of participants

Vera Angelova
Institute of Information and
Communication Technologies
Bulgarian Academy of Sciences
Akad. G. Bonchev, Str., Bl. 2
1113 Sofia, Bulgaria
vangelova@iit.bas.bg

Atanas Z. Atanasov
"Angel Kanchev" University of Ruse
8 Studentska Str.
7017 Ruse, Bulgaria

Todor Balabanov
Institute of Information and
Communication Technologies
Bulgarian Academy of Sciences
Acad. G. Bonchev Str., Bl. 2, office 514
1113 Sofia, Bulgaria
todor.balabanov@iict.bas.bg

Ivan Blagoev
Institute of Information and
Communication Technologies
Bulgarian Academy of Sciences
Akad. G. Bonchev, Str., Bl. 2
1113 Sofia, Bulgaria
ivan.blagoev@iict.bas.bg

Vilislav Boutchaktchiev
University of National and World
Economy
1700 Sofia, Bulgaria
vboutcha@unwe.bg
and
Institute of Mathematics and Informatics
Bulgarian Academy of Sciences
Acad. G. Bonchev Str., Bl. 8
1113 Sofia, Bulgaria

Stefan Bushev
Institute of Metal Science, Equipment
and Technologies "Acad. A. Balevsci"
with Haydroaerodinamics Centre
Bulgarian Academy of Sciences
67 Shipchenski prohod Str.
1574 Sofia, Bulgaria

Maria Datcheva
Institute of Mechanics
Bulgarian Academy of Sciences
Acad. G. Bonchev Str., Bl. 4
1113 Sofia, Bulgaria
datcheva@imbm.bas.bg

Ivan Georgiev
Institute of Information and
Communication Technologies
Bulgarian Academy of Sciences
Acad. G. Bonchev Str., Bl. 2
and
Institute of Mathematics and Informatics
Bulgarian Academy of Sciences
Acad. G. Bonchev Str., Bl. 8
1113 Sofia, Bulgaria

Slavi Georgiev
"Angel Kanchev" University of Ruse
8 Studentska Str.
7017 Ruse, Bulgaria
georgiev.slavi.94@gmail.com

Ivan Hristov
Faculty of Mathematics and Informatics
Sofia University "St. Kliment Ohridski"
5 J. Bourchier Blvd.
1164 Sofia, Bulgaria
christov_ivan@abv.bg

Clemens Hofreither
Johann Radon Institute for Computational
and Applied Mathematics
4040 Linz, Austria

Tihomir B. Gyulov
Department of Mathematics,
"Angel Kanchev" University of Ruse
6 Studentska Str.
7017 Ruse, Bulgaria
tgulov@uni-ruse.bg

Roumen Iankov
Institute of Mechanics
Bulgarian Academy of Sciences
Acad. G. Bonchev Str., Bl. 4
1113 Sofia
iankovr@abv.bg

Mario T. Iliev
Faculty of Physics
Sofia University "St. Kliment Ohridski"
5 J. Bourchier Blvd.
1164 Sofia, Bulgaria

Nevena Ilieva
Institute of Information and
Communication Technologies
Bulgarian Academy of Sciences
Acad. G. Bonchev Str, Bl. 25A
1113 Sofia, Bulgaria
nevena.ilieva@parallel.bas.bg
and
Institute of Mathematics and Informatics
Bulgarian Academy of Sciences
Acad. G. Bonchev Str., Bl. 8
1113 Sofia, Bulgaria

Ivan P. Jordanov
University of National and World
Economy
Studentski Grad, UNWE - office 2087
1700 Sofia, Bulgaria
and
Institute of Mechanics,
Bulgarian Academy of Sciences
Acad. G. Bonchev Str.,Bl. 4
1113 Sofia, Bulgaria
jordanovip@gmail.com

Juri Kandilarov
"Angel Kanchev" University of Ruse
8 Studentska Str.
7017 Ruse, Bulgaria
ukandilarov@uni-ruse.bg

Julius Kaplunov
School of Computing and Mathematics
Keele University
Keele ST5 5BG, UK
j.kaplunov@keele.ac.uk

Miglena Koleva
"Angel Kanchev" University of Ruse
6 Studentska Str.
7017 Ruse, Bulgaria
mkoleva@uni-ruse.bg

Hristo Kostadinov
Institute of Mathematics and Informatics
Bulgarian Academy of Sciences
Acad. G. Bonchev Str., Bl. 8
1113 Sofia, Bulgaria

Elena Lilkova
Institute of Information and
Communication Technologies
Bulgarian Academy of Sciences
Acad. G. Bonchev Str., Bl. 25A
1113 Sofia, Bulgaria
elena.lilkova@iict.bas.bg

Alexander B. Manov
Faculty of Mathematics and Informatics
Sofia University "St. Kl. Ohridski"
5 J. Bourchier Blvd.
1164 Sofia, Bulgaria
aleksander.manov@gmail.com

Svetozar Margenov
Institute of Information and
Communication Technologies
Bulgarian Academy of Sciences
Acad. G. Bonchev Str., Bl. 25A
1113 Sofia, Bulgaria
margenov@parallel.bas.bg

Zlatogor Minchev
Institute of Information and
Communication Technologies
Bulgarian Academy of Sciences
Acad. G. Bonchev Str., Bl. 25A
1113 Sofia, Bulgaria
zlatogor.minchev@gmail.com

Tzvetan Ostromsky
Institute of Information and
Communication Technologies
Bulgarian Academy of Sciences
Acad. G. Bonchev Str., Bl. 25A
1113 Sofia, Bulgaria
ceco@parallel.bas.bg

Xubiao Peng
Centre for Quantum Technology
Research
Beijing Institute of Technology
China
xubiaopeng@bit.edu.cn

Peicho Petkov
Faculty of Physics
Sofia University "St. Kl. Ohridski"
5 J. Bourchier Blvd.
1164 Sofia, Bulgaria
peicho@phys.uni-sofia.bg

Angela Slavova
Institute of Mathematics and Informatics
Bulgarian Academy of Sciences
Acad. G. Bonchev Str., Bl. 8
1113 Sofia, Bulgaria

Margarita Terziyska
University of Food Technology
26 Maritsa Blvd.
Plovdiv, Bulgaria
mterziyska@uft-plovdiv.bg

Nikolay K. Vitanov
Institute of Mechanics
Bulgarian Academy of Sciences
Acad. G. Bonchev Str.,Bl. 4
1113 Sofia, Bulgaria
vitanov@imbm.bas.bg

Krassimira Vlachkova
Faculty of Mathematics and Informatics
Sofia University "St. Kl. Ohridski"
5 J. Bourchier Blvd.
1164 Sofia, Bulgaria
krassivl@fmi.uni-sofia.bg

Lubin Vulkov
Ruse University
6 Studentska St
7017 Ruse, Bulgaria
lvalkov@uni-ruse.bg

Maria Zarcheva
Faculty of Mathematics and Informatics
Sofia University "St. Kl. Ohridski"
5 J. Bourchier Blvd.
1164 Sofia, Bulgaria
mzarcheva@fmi.uni-sofia.bg